INSIDE TRACK with **Ken Karnofsky,** MathWorks | 28

Cutting-Edge Amplifiers for Today's Tech | 35

Testing Circuit Materials | 39

microwaves&rf

AUGUST 2016 TRUSTED ENGINEERING RESOURCE FOR OVER 50 YEARS www.mwrf.com

AMPLIFIERS & OSCILLATORS ISSUE

VSTs: The New Generation

p | 65

$10.00 Powered by Penton

Periodicals Postage Paid • USPS 100 Approved Poly

VOLUME 55, ISSUE 8

In This Issue

65

FEATURES

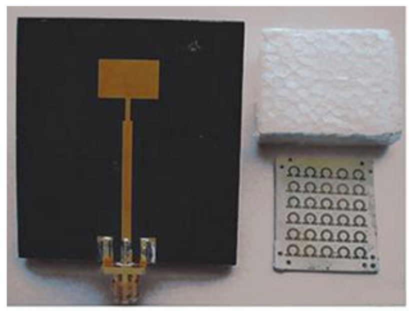

46

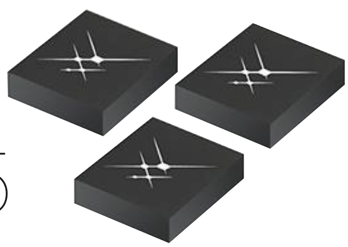

35

INDUSTRY TRENDS & ANALYSIS

PRODUCT TECHNOLOGY

NEWS & COLUMNS

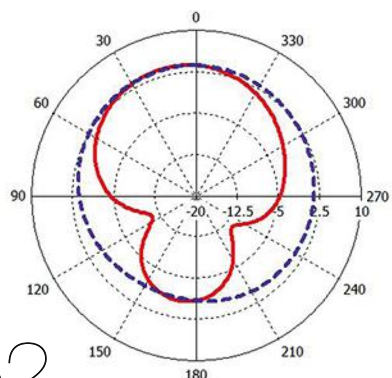

52

JOIN US ONLINE

follow us @MicrowavesRF

become a fan at facebook.com/microwavesRF

60

BETTER COMMUNICATION SOLUTIONS

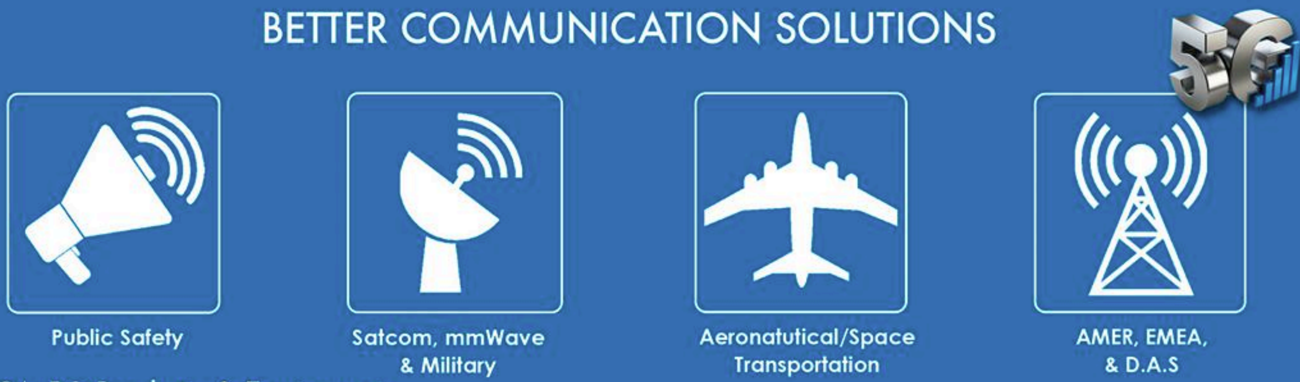

MECA 5G Products & Equipment

MECA Electronics designs and manufactures an extensive line of RF/Microwave Equipment and Components with industry leading performance including D.A.S. Equipment, Low PIM Products, supports 5G & Millimeter-Wave, Power Dividers & Combiners, Directional & Hybrid Couplers, Fixed & Variable Attenuators, RF Terminations, Circulators/Isolators, DC Blocks & Bias Tees, Adapters & Jumpers. Models available in industry common connector styles: N, SMA, 2.92mm, TNC, BNC, 7/16, 4.1/9.5 & 4.3/10.0 DIN as well as QMA, Reverse Polarity SMA, TNC and various mounting solutions. Since 1961 MECA Electronics (Microwave Equipment & Components of America) has served the RF/Microwave industry with equipment and passive components covering Hz to 40 GHz. MECA is a privately held ISO9001:2008 Certified, global designer and manufacturer for the communications industry with products manufactured in the United States of America We stock products so that you do not need to.

e-MECA.com
Since 1961

MECA Electronics, Inc.

Microwave Equipment & Components of America

The Professional's Choice for RF/Microwave Passive Components

459 E. Main St., Denville, NJ 07834

Tel: 973-625-0661 • Fax: 973-625-9277 • Sales@e-MECA.com

iBwave

MACOM GaN...Delivered

Enabling RF Energy with Leading Efficiency & Gain

MACOM GaN Delivers Outstanding Performance

	LDMOS	MACOM GaN on Silicon	Benefits
Power Amp Efficiency “>2GHz”	–	> 10% Improvement	Lower Operating Costs, Simpler Cooling
Power Density	1-1.5 W/mm	4-6 W/mm	Smaller Footprint and Lower Costs
Matching	Difficult	Easy	Time-to-Market and Smaller Footprint
Supply Chain	8”	6” & 8”	Capacity and Surge Capability
Cost	Silicon	Silicon	Competitive Bill of Materials
Support all ISM Brands	Limited to 2.45 GHz	Can be used at >2.45 GHz	Broader Choice for Your Applications

on microwaves&rf.com

ACCESSORIES ADD UP TO BETTER MEASUREMENTS

http://mwrf.com/blog/accessories-add-better-measurements

Purchasing a test instrument is a major investment, and measurements don't begin and end with the instrument—they may also depend on such things as instrument cables. In his latest blog, Tech Editor Jack Browne asks, "What kind of test accessories can be beneficial, and why?"

BEHIND INFINEON'S WOLFSPEED DEAL

http://mwrf.com/active-components/infineon-buys-crees-wolfspeed-gallium-nitride-devices

In a surprise reshuffling of the market for advanced semiconductor materials, Infineon Technologies announced that it has agreed to buy Wolfspeed, the former division of Cree that makes power and radio frequency chips. What will that mean for the semiconductor market?

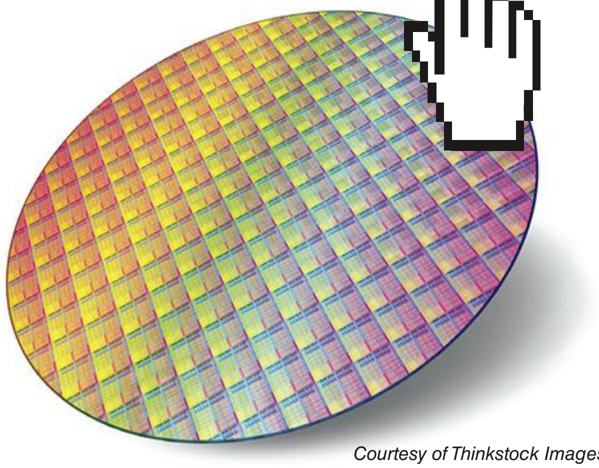

Courtesy of Thinkstock Images

GaN VERSUS GaAs

http://mwrf.com/materials/what-s-difference-between-gan-and-gaas

GaN has emerged as the leading semiconductor material for high-power microwave switches and amplifiers, although GaAs is still the material of choice for low noise.

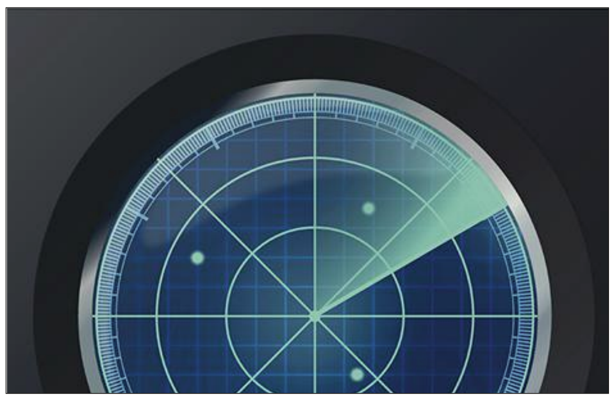

Courtesy of Thinkstock Images

RADAR REACHES NEW TERRITORIES

http://mwrf.com/systems/radar-technology-encroaches-up-on-new-territories

As radar systems utilize more advanced technology, companies must respond with the simulation and test products needed to both design and test modern radar systems.

join us online

twitter.com/MicrowavesRF facebook.com/microwavesrf

Editorial

CHRIS DEMARTINO

Technical Editor

chris.demartinol@penton.com

5G Prepares for Takeoff

Last year, I wrote a column titled "Looking Ahead to 5G," which discussed the great expectations that many have for the standard—never mind the fact its details were (and still are) yet to be determined. Recently, however, major news came forth from the Federal Communications Commission (FCC) that will set the stage for 5G development. The FCC unanimously voted to open up nearly 11 GHz of high-frequency spectrum, unlocking frequencies above 24 GHz for future 5G networks. This news means that the U.S. is the first nation to allow spectrum above 24 GHz to be available for 5G.

The unanimous voting opens up spectrum in the 28-, 37-, and 39-GHz frequency bands, as well as the unlicensed 64- to 71-GHz band. Following the announcement, the Obama administration pledged its support, announcing a $400 million research initiative. Led by the National Science Foundation (NSF), this initiative seeks to build four city-scale advanced wireless testing platforms.

All of this news demonstrates why 5G is such a hot topic nowadays. The interesting part of all of this is the fact that nobody exactly knows what the standard will be. Although the news from the FCC is a major step toward 5G reality, much work still needs to be done for 5G to actually be defined. Of course, everyone wants faster speeds. But exactly how will 5G enable it? That question will need to be answered.

One thing is clear: The RF/microwave industry is gearing up for 5G. Keysight Technologies (www.keysight.com), for example, just introduced the Signal Optimizer software, which is a tool for 5G candidate waveform signal creation and analysis. The company's 5G channel-sounding reference solution is another example of Keysight's focus on this area. Many other companies have their eyes on 5G, as well. With all of the anticipation surrounding 5G, expect to continue hearing many announcements in the days to come. mw

AUGUST | 2016

microwaves&rf

Powered by Penton

EDITORIAL

CONTENT DIRECTOR: **NANCY K. FRIEDRICH** nancy.friedrich@penton.com
TECHNICAL CONTRIBUTOR: **JACK BROWNE** jack.browne@penton.com
TECHNICAL ENGINEERING EDITOR: **CHRIS DeMARTINO** chris.demartino@penton.com
CONTENT PRODUCTION DIRECTOR: **MICHAEL BROWNE** michael.browne@penton.com
PRODUCTION EDITOR: **JEREMY COHEN** jeremy.cohen@penton.com
CONTENT PRODUCTION SPECIALIST: **ROGER ENGELKE** roger.engelke@penton.com
CONTENT OPTIMIZATION SPECIALIST: **WES SHOCKLEY** wes.shockley@penton.com
ASSOCIATE CONTENT PRODUCER: **LEAH SCULLY** leah.scully@penton.com
ASSOCIATE CONTENT PRODUCER: **JAMES MORRA** james.morra@penton.com

ART DEPARTMENT

GROUP DESIGN DIRECTOR: **ANTHONY VITOLO** tony.vitolo@penton.com
SENIOR ARTIST: **JIM MILLER** jim.miller@penton.com
CONTRIBUTING ART DIRECTOR **RANDALL L. RUBENKING** randall.rubenking@penton.com

PRODUCTION

GROUP PRODUCTION MANAGER: **CAREY SWEETEN** carey.sweeten@penton.com
PRODUCTION MANAGER: **VICKI MCCARTY** vicki.mccarty@penton.com
CLASSIFIED PRODUCTION COORDINATOR: **LINDA SARGENT** linda.sargent@penton.com

AUDIENCE MARKETING

USER MARKETING DIRECTOR: **BRENDA ROODE** brenda.roode@penton.com
USER MARKETING MANAGER: **DEBBIE BRADY** debbie.brady@penton.com
FREE SUBSCRIPTION/STATUS OF SUBSCRIPTION/ADDRESS CHANGE/MISSING BACK ISSUES
T | 866.505.7173 microwaves&RF@halldata.com **F** | 847.763.9673

SALES & MARKETING

MANAGING DIRECTOR: **TRACY SMITH** **T** | 913.967.1324 **F** | 913.514.6881
tracy.smith@penton.com

REGIONAL SALES REPRESENTATIVES

GREGORY MONTGOMERY **T** | 480.254.5540 gregory.montgomery@penton.com
AK, CA, CO, ID, MT, ND, NV, OR, SD, UT, WA, WI, WY, W/CANADA: **JAMIE ALLEN** **T** | 415.608.1959
F | 913.514.3667 jamie.allen@penton.com
AL, AR, IA, IL, IN, KS, KY, LA, MI, MN, MO, MS, NE, OH, OK, TN: **PAUL MILNAMOW**
T | 312.840.8462 paul.milnamow@penton.com
CT, DE, FL, GA, MA, MD, ME, NC, NH, NJ, NY, RI, PA, SC, VA, VT, WV, EASTERN CANADA:
SHANNON ALO-MENDOSA **T** | 978.501.7303 Shannon.alo-mendosa@penton.com

INTERNATIONAL SALES

GERMANY, AUSTRIA, SWITZERLAND: **CHRISTIAN HOELSCHER** **T** | 011.49.89.95002778
christian.hoelscher@husonmedia.com
BELGIUM, NETHERLANDS, LUXEMBURG UNITED KINGDOM, SCANDINAVIA, FRANCE, SPAIN, PORTUGAL:
JAMES RHOADES-BROWN **T** | +011 44 1932 564999 **M** | +011 44 1932 564998
james.rhoadesbrown@husonmedia.com
PAN-ASIA: **HELEN LAI** **T** | 886 2-2727 7799 helen@twoway-com.com

PLEASE SEND INSERTION ORDERS TO: orders@penton.com
PENTON REPRINTS: **WRIGHT'S MEDIA** **T** | 877.652.5295 penton@wrightsmedia.com
CIRCULATION: **CUSTOMER SERVICE** **T** | 866.505.7173 **F** | 847.763.9673 microwaves&rf@halldata.com

LIST RENTALS:
SMARTREACH CLIENT SERVICES MANAGER: **DAVID SICKLES** **T** | (212) 204 4379
david.sickles@penton.com

ONLINE

PRODUCT DEVELOPMENT DIRECTOR: **RYAN MALEC** ryan.malec@penton.com

DESIGN ENGINEERING & SOURCING GROUP

EXECUTIVE DIRECTOR OF CONTENT AND USER ENGAGEMENT: **NANCY K. FRIEDRICH**
GROUP DIRECTOR OF OPERATIONS: **CHRISTINA CAVANO**
GROUP DIRECTOR OF MARKETING: **JANE COOPER**

PENTON

CHIEF EXECUTIVE OFFICER: **DAVID KIESELSTEIN** david.kieselstein@penton.com
CHIEF FINANCIAL OFFICER: **NICOLA ALLAIS** nicola.allais@penton.com
INDUSTRY GROUP, PRESIDENT: **PAUL MILLER** paul.miller@penton.com
1166 AVENUE OF THE AMERICAS, 10TH FLOOR NEW YORK, NY 10036 **T** | 212.204.4200

Penton

Electronic Design | Machine Design | Microwaves & RF | Medical Design | Source ESB | Hydraulics & Pneumatics | Global Purchasing | Distribution Resource | Power Electronics | Defense Electronics | Electronic Design Europe | Engineering TV

RF Amplifiers and Sub-Assemblies for Every Application

Delivery from Stock to 2 Weeks ARO from the catalog or built to your specifications!

- Competitive Pricing & Fast Delivery
- Military Reliability & Qualification
- Various Options: Temperature Compensation, Input Limiter Protection, Detectors/TTL & More
- Unconditionally Stable (100% tested)

ISO 9001:2000 and AS9100B CERTIFIED

OCTAVE BAND LOW NOISE AMPLIFIERS

Model No.	Freq (GHz)	Gain (dB) MIN	Noise Figure (dB)	Power-out @ P1-dB	3rd Order ICP	VSWR
CA01-2110	0.5-1.0	28	1.0 MAX, 0.7 TYP	+10 MIN	+20 dBm	2.0:1
CA12-2110	1.0-2.0	30	1.0 MAX, 0.7 TYP	+10 MIN	+20 dBm	2.0:1
CA24-2111	2.0-4.0	29	1.1 MAX, 0.95 TYP	+10 MIN	+20 dBm	2.0:1
CA48-2111	4.0-8.0	29	1.3 MAX, 1.0 TYP	+10 MIN	+20 dBm	2.0:1
CA812-3111	8.0-12.0	27	1.6 MAX, 1.4 TYP	+10 MIN	+20 dBm	2.0:1
CA1218-4111	12.0-18.0	25	1.9 MAX, 1.7 TYP	+10 MIN	+20 dBm	2.0:1
CA1826-2110	18.0-26.5	32	3.0 MAX, 2.5 TYP	+10 MIN	+20 dBm	2.0:1

NARROW BAND LOW NOISE AND MEDIUM POWER AMPLIFIERS

Model No.	Freq (GHz)	Gain (dB) MIN	Noise Figure (dB)	Power-out @ P1-dB	3rd Order ICP	VSWR
CA01-2111	0.4 - 0.5	28	0.6 MAX, 0.4 TYP	+10 MIN	+20 dBm	2.0:1
CA01-2113	0.8 - 1.0	28	0.6 MAX, 0.4 TYP	+10 MIN	+20 dBm	2.0:1
CA12-3117	1.2 - 1.6	25	0.6 MAX, 0.4 TYP	+10 MIN	+20 dBm	2.0:1
CA23-3111	2.2 - 2.4	30	0.6 MAX, 0.45 TYP	+10 MIN	+20 dBm	2.0:1
CA23-3116	2.7 - 2.9	29	0.7 MAX, 0.5 TYP	+10 MIN	+20 dBm	2.0:1
CA34-2110	3.7 - 4.2	28	1.0 MAX, 0.5 TYP	+10 MIN	+20 dBm	2.0:1
CA56-3110	5.4 - 5.9	40	1.0 MAX, 0.5 TYP	+10 MIN	+20 dBm	2.0:1
CA78-4110	7.25 - 7.75	32	1.2 MAX, 1.0 TYP	+10 MIN	+20 dBm	2.0:1
CA910-3110	9.0 - 10.6	25	1.4 MAX, 1.2 TYP	+10 MIN	+20 dBm	2.0:1
CA1315-3110	13.75 - 15.4	25	1.6 MAX, 1.4 TYP	+10 MIN	+20 dBm	2.0:1
CA12-3114	1.35 - 1.85	30	4.0 MAX, 3.0 TYP	+33 MIN	+41 dBm	2.0:1
CA34-6116	3.1 - 3.5	40	4.5 MAX, 3.5 TYP	+35 MIN	+43 dBm	2.0:1
CA56-5114	5.9 - 6.4	30	5.0 MAX, 4.0 TYP	+30 MIN	+40 dBm	2.0:1
CA812-6115	8.0 - 12.0	30	4.5 MAX, 3.5 TYP	+30 MIN	+40 dBm	2.0:1
CA812-6116	8.0 - 12.0	30	5.0 MAX, 4.0 TYP	+33 MIN	+41 dBm	2.0:1
CA1213-7110	12.2 - 13.25	28	6.0 MAX, 5.5 TYP	+33 MIN	+42 dBm	2.0:1
CA1415-7110	14.0 - 15.0	30	5.0 MAX, 4.0 TYP	+30 MIN	+40 dBm	2.0:1
CA1722-4110	17.0 - 22.0	25	3.5 MAX, 2.8 TYP	+21 MIN	+31 dBm	2.0:1

ULTRA-BROADBAND & MULTI-OCTAVE BAND AMPLIFIERS

Model No.	Freq (GHz)	Gain (dB) MIN	Noise Figure (dB)	Power-out @ P1-dB	3rd Order ICP	VSWR
CA0102-3111	0.1-2.0	28	1.6 Max, 1.2 TYP	+10 MIN	+20 dBm	2.0:1
CA0106-3111	0.1-6.0	28	1.9 Max, 1.5 TYP	+10 MIN	+20 dBm	2.0:1
CA0108-3110	0.1-8.0	26	2.2 Max, 1.8 TYP	+10 MIN	+20 dBm	2.0:1
CA0108-4112	0.1-8.0	32	3.0 MAX, 1.8 TYP	+22 MIN	+32 dBm	2.0:1
CA02-3112	0.5-2.0	36	4.5 MAX, 2.5 TYP	+30 MIN	+40 dBm	2.0:1
CA26-3110	2.0-6.0	26	2.0 MAX, 1.5 TYP	+10 MIN	+20 dBm	2.0:1
CA26-4114	2.0-6.0	22	5.0 MAX, 3.5 TYP	+30 MIN	+40 dBm	2.0:1
CA618-4112	6.0-18.0	25	5.0 MAX, 3.5 TYP	+23 MIN	+33 dBm	2.0:1
CA618-6114	6.0-18.0	35	5.0 MAX, 3.5 TYP	+30 MIN	+40 dBm	2.0:1
CA218-4116	2.0-18.0	30	3.5 MAX, 2.8 TYP	+10 MIN	+20 dBm	2.0:1
CA218-4110	2.0-18.0	30	5.0 MAX, 3.5 TYP	+20 MIN	+30 dBm	2.0:1
CA218-4112	2.0-18.0	29	5.0 MAX, 3.5 TYP	+24 MIN	+34 dBm	2.0:1

LIMITING AMPLIFIERS

Model No.	Freq (GHz)	Input Dynamic Range	Output Power Range Psat	Power Flatness dB	VSWR
CLA24-4001	2.0 - 4.0	-28 to +10 dBm	+7 to +11 dBm	+/- 1.5 MAX	2.0:1
CLA26-8001	2.0 - 6.0	-50 to +20 dBm	+14 to +18 dBm	+/- 1.5 MAX	2.0:1
CLA712-5001	7.0 - 12.4	-21 to +10 dBm	+14 to +19 dBm	+/- 1.5 MAX	2.0:1
CLA618-1201	6.0 - 18.0	-50 to +20 dBm	+14 to +19 dBm	+/- 1.5 MAX	2.0:1

AMPLIFIERS WITH INTEGRATED GAIN ATTENUATION

Model No.	Freq (GHz)	Gain (dB) MIN	Noise Figure (dB)	Power-out @ P1-dB	Gain Attenuation Range	VSWR
CA001-2511A	0.025-0.150	21	5.0 MAX, 3.5 TYP	+12 MIN	30 dB MIN	2.0:1
CA05-3110A	0.5-5.5	23	2.5 MAX, 1.5 TYP	+18 MIN	20 dB MIN	2.0:1
CA56-3110A	5.85-6.425	28	2.5 MAX, 1.5 TYP	+16 MIN	22 dB MIN	1.8:1
CA612-4110A	6.0-12.0	24	2.5 MAX, 1.5 TYP	+12 MIN	15 dB MIN	1.9:1
CA1315-4110A	13.75-15.4	25	2.2 MAX, 1.6 TYP	+16 MIN	20 dB MIN	1.8:1
CA1518-4110A	15.0-18.0	30	3.0 MAX, 2.0 TYP	+18 MIN	20 dB MIN	1.85:1

LOW FREQUENCY AMPLIFIERS

Model No.	Freq (GHz)	Gain (dB) MIN	Noise Figure dB	Power-out @ P1-dB	3rd Order ICP	VSWR
CA001-2110	0.01-0.10	18	4.0 MAX, 2.2 TYP	+10 MIN	+20 dBm	2.0:1
CA001-2211	0.04-0.15	24	3.5 MAX, 2.2 TYP	+13 MIN	+23 dBm	2.0:1
CA001-2215	0.04-0.15	23	4.0 MAX, 2.2 TYP	+23 MIN	+33 dBm	2.0:1
CA001-3113	0.01-1.0	28	4.0 MAX, 2.8 TYP	+17 MIN	+27 dBm	2.0:1
CA002-3114	0.01-2.0	27	4.0 MAX, 2.8 TYP	+20 MIN	+30 dBm	2.0:1
CA003-3116	0.01-3.0	18	4.0 MAX, 2.8 TYP	+25 MIN	+35 dBm	2.0:1
CA004-3112	0.01-4.0	32	4.0 MAX, 2.8 TYP	+15 MIN	+25 dBm	2.0:1

CIAO Wireless can easily modify any of its standard models to meet your "exact" requirements at the Catalog Pricing.

Visit our web site at **www.ciaowireless.com** for our complete product offering.

Ciao wireless

Ciao Wireless, Inc. 4000 Via Pescador, Camarillo, CA 93012

Tel (805) 389-3224 Fax (805) 389-3629 sales@ciaowireless.com

DON'T MISPLACE THOSE DECIMAL POINTS

I apologize if I am adding to a stream of e-mails to you saying the same thing. In the July issue of *Microwaves & RF*, you wrote a piece, "What's the difference between GaN and GaAs," meant to be an engineering comparison of two of the more popular high-frequency semiconductor materials. In that piece, you wrote "GaN also has a much higher relative dielectric constant, at 9.0, than that of GaAs, at 1.28, allowing for fabrication much higher-valued capacitors."

In truth, GaAs has a higher dielectric constant than GaN, at about 12.9 and not 1.28, and you don't make high-value capacitors with the base substrate as the dielectric material.

Andy Hughes
Solutions Architect—
Northeastern U.S. & Canada
National Instruments
(AWR Group)

EDITOR'S NOTE

We always appreciate your feedback, Andy—don't ever be shy about writing. Yes, I was trying to point out some quick differences between GaAs and GaN and, as you noted, couldn't cover all the ground. In looking at the mistake you pointed out, I realized that even the best spell-checking software can't make up for tired typing fingers. It was a case of my jotting down specifications about GaN and GaAs substrate materials and putting the decimal point in the wrong place: What should have been printed as 12.8 came out as 1.28 in my initial notes, leading me to report the incorrect value in the final story.

My apologies to you and to all our readers, and my gratitude to you for taking the time to point out the error. This kind of interaction with readers is invaluable to any editor; it helps to make us more careful in the future, and try to do better jobs. As the story pointed out, there are many differences between GaN and GaAs, but dielectric constant was not one of them.

Jack Browne
Technical Contributor

Microwaves & RF welcomes mail from its readers. The magazine reserves the right to edit letters appearing in "Feedback." Address letters to:

Jack Browne
Technical Contributor
jack.browne@penton.com

Nancy Friedrich
Content Director
nancy.friedrich@penton.com

News

SAMSUNG MAKES STRIDES in Shrinking 5G Antennas

Samsung Electronics said it has made smaller and more efficient parts for fifth-generation, or 5G, wireless networks, tackling one of the trickier problems with new wireless standards. The new parts include miniaturized antennas and power amplifiers, both of which can be used inside 5G base stations and devices like smartphones.

The new parts underline the two-front battle that chipmakers and wireless equipment makers are fighting to develop not only 5G standards, but also the hardware to exploit it. 5G could prove fast enough to download entire movies in seconds or replace fiber optics in linking access points to the internet.

"We are very focused on developing technologies that improve and accelerate the realization of a new generation of mobile networks and devices," said Paul Kyungwhoon Cheun, who directs 5G projects as the executive vice president of Samsung's Next Generation Business division.

In a statement, the South Korean chipmaker described the new devices as "5G-ready," but declined to say when they might be available. According to Samsung, the antennas and power amplifiers work with 28-GHz millimeter waves, which analysts believe will be a major channel for data flowing through 5G.

The new antennas combine dozens of elements into a module less than 1 mm thick, making them ideal for small-cell base stations and user devices like smartphones or tablets. Driving each antenna are the new power amplifiers, which can double the output power of signals over earlier parts. According to Samsung, they are also around 50% more power-efficient than other prototypes made for 5G.

According to Kungwhoon Cheun, the devices have to be small and highly efficient in order to work with 5G infrastructure. Since millimeter waves can only travel short distances

(continued on p. 26)

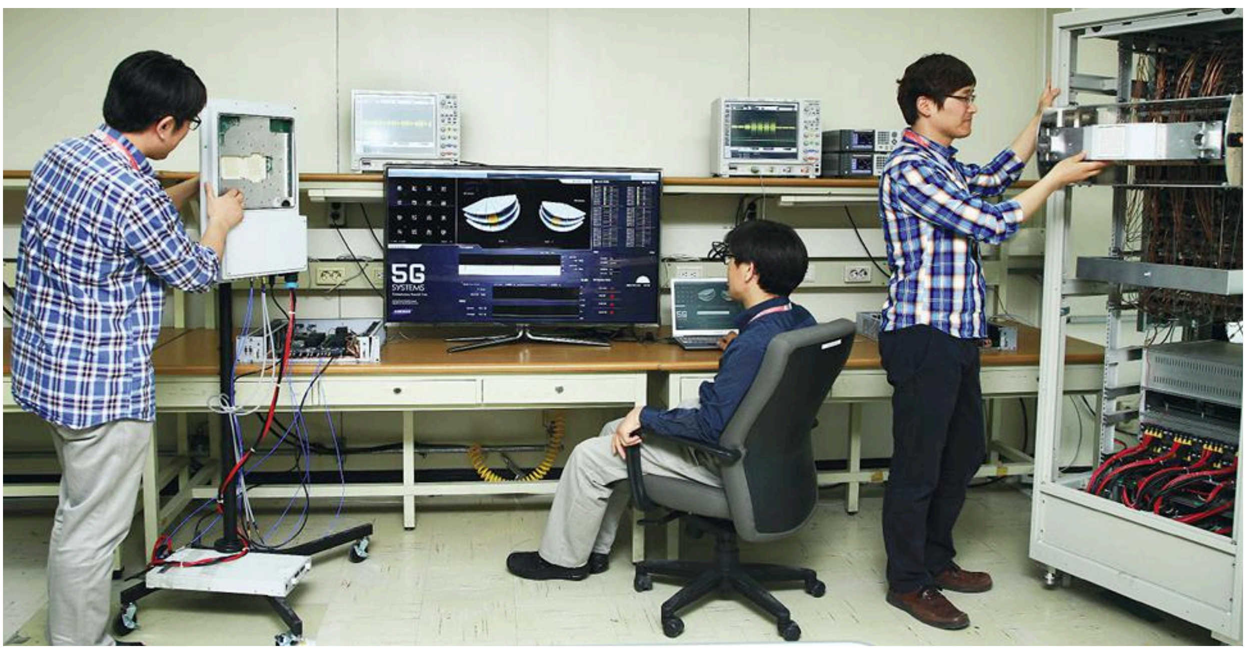

Samsung engineers, in 2013, set up tests for the chipmaker's early 5G equipment. More recent advances have produced smaller and more efficient parts for 5G wireless networks. *(Image courtesy of Samsung)*

FACEBOOK'S TINY CELL STATION
Eyes the Remote and Rural

FOR YEARS, FACEBOOK has handed out its software to developers in attempts to quickly refine its internet services. But the social media company has also used this open-source model to steer hardware markets in new directions. Its efforts began in 2012 with the Open Compute Project, in which Facebook shared its custom server designs with hardware makers like Intel and Hewlett-Packard.

By partnering with hardware and cloud computing companies, Facebook bet that the new equipment would be easier to reprogram and to expand its sprawling data centers. Lately, Facebook has applied this model to wireless hardware, in an attempt to bring cellular and internet service to remote locations that might not have access to the social media site.

Facebook recently revealed the plan's latest building block: a new device calledOpenCellular that allows wireless carriers to bring connectivity to places lying outside the reach of cell towers. The small device, which can be attached to telephone poles or tree trunks, contains processors and storage capacity to support wireless networks.

According to Facebook, the hardware inside can support anything from simple 2G cellular networks to significantly faster 4G and Wi-Fi services. The device contains a general baseband computing system, in addition to radio hardware with an integrated RF front-end. With both parts, OpenCellular can be configured as an access point—or a cellular network that lets people make local calls and texts.

According to Facebook, the new device is aimed at extending broadband service to the roughly 4 billion people isolated from the internet at the end of 2015. The company estimated that about 10% of the world's population lived outside the range of cellular connectivity in 2015.

"One of the reasons the expansion of cellular networks has stalled is that the ecosystem is constrained," said Kashif Ali, an engineer working on the project, in a blog post. OpenCellular, on the other hand, includes "architectural and design improvements that would result in lower costs associated with the civil and support infrastructure."

It almost resembles a small cell, said Sue Rudd, an analyst at research firm Strategy Analytics, who has followed Facebook's and Google's wireless projects. Though the equipment itself might be lower in cost and more energy-efficient, she said, the biggest cost lies in the infrastructure surrounding the device and the task of connecting mobile phones to the internet.

The OpenCellular device. *(Image courtesy of Facebook)*

Traditional wireless carriers have eschewed rural towns and villages precisely for that reason. The cost involved with building infrastructure can make serving these places unaffordable. Instead, wireless carriers and equipment makers like Ericsson and Huawei have typically focused on improving service in cities and heavily populated areas.

OpenCellular stands out because it will be freely available to developers. Facebook said that members of its Telecom Infra Project, which aims to develop new kinds of wireless hardware with telecommunications companies, will have access to the device. Some of the largest wireless carries in Germany and Korea, in addition to equipment maker Nokia Networks, have signed onto the project. If these companies make OpenCellular part of

(continued on p. 24)

U.S. REGULATORS OPEN
New Millimeter Wave Spectrum

THE WIRELESS INDUSTRY is lighting a fire underneath the Federal Communications Commission (FCC) to open more spectrum for fifth-generation, or 5G, wireless networks. The influence of wireless companies, which are testing 5G systems out in the field, is obvious in its latest spectrum auction. The agency is trying to raise around $84.6 billion for broadcast television spectrum repurposed for mobile communications.

Now the agency is opening spectrum never used before. In July, it approved a proposal that will break ground in frequency bands above 28 GHz, which are also known as millimeter waves. Regulators voted unanimously in favor of the new rules.

Wireless carriers, chipmakers, and equipment manufacturers are piling into the millimeter wave spectrum. In cities, researchers are using high-frequency bands and small cells to send data into mobile devices, instead of the low-frequency bands and large cell stations driving 4G networks. The higher-frequency bands are enabling faster response times, capacity to support massive amounts of devices, and download speeds over 10 times faster than 4G. Among the services possible with 5G networks are video streaming for virtual and augmented reality and connecting billions of devices in the Internet of Things.

The rule-making is the latest attempt by regulators to keep pace with 5G testing in the United States. Last month, for example, Sprint tested a wireless network with 4 gigabit per second downloads at the Copa America soccer tournament in Philadelphia. Verizon has already completed its 5G radio specification, while Samsung is making millimeter-wave parts for smartphones and cellular equipment. The first networks that the average person can access are expected in 2020.

According to the new rules, nearly 11 GHz of high-frequency spectrum will be opened for mobile and fixed wireless broadband. The licensed bands include 27.5 to 28.35 GHz, 37 to 38.6 GHz, and 38.6 to 40 GHz. The rules also introduced a new band of unlicensed spectrum between 64 and 71 GHz.

"By opening up these higher-frequency bands, we are making available over four times the total amount of licensed spectrum currently available for mobile," Tom Wheeler, the FCC chairman, said in a statement. The new spectrum bands are 200 megahertz in width, as opposed to current blocks of low-band spectrum, which are usually 5 to 10 megahertz wide.

The new rules make the United States the first country to open millimeter-wave spectrum, the agency said. The rules are more flexible than those established for 4G networks, allowing companies to share spectrum for fixed and mobile broadband, as well as satellite and ground communications. "We are setting flexible rules that will allow the market to best determine how the technology will evolve, without having to ask our permission," Wheeler said. "Without question, 5G is a national priority."

While the voting was unanimous, several members voiced reservations. For example, commissioner Michael O'Reilly was not satisfied with the amount of spectrum released. "I sought to include more bands," he said, citing bands 40-42 GHz, 42.5 to 43.5 GHz, and 45.5 to 47 GHz in his testimony.

Following the vote, the U.S. government said that it would establish the Advanced Wireless Research Initiative, which will have $400 million in funding. The program will get $50 million over the next five years from the National Science Foundation and wireless technology companies including Qualcomm, Intel, and Keysight Technologies. The National Science Foundation will commit another $350 million over the next seven years in wireless research.

The funds will be applied to test systems in four cities around the United States. Each system will include a network of software-defined radio antennas, which will mimic existing cellular infrastructure. With the systems, researchers and wireless companies will be able to test and refine wireless components and software algorithms. ■

NARROWBAND IOT STANDARD Gets Stamp of Approval

FOR YEARS, the 3G Partnership Project has faced skepticism about its role within the Internet of Things and how it might approach the difficult task of connecting millions of simple wireless devices. More recently, though, the organization has defied the suggestion that cellular networks are not meant for tiny electronic devices, buckling down on standards that are gentler on the batteries inside sensors and other electronics.

Those efforts are finally bearing fruit, with the organization recently saying that it has finished laying out a new wireless IoT standard. The new technology is known as Narrowband-IoT and joins several others under the umbrella of the 4G LTE specification.

(Image courtesy of Monicaodo, Thinkstock)

Though it uses the same spectrum and signal processing technology, Narrowband-IoT makes an important change to its underlying cellular standard. NB-IoT is not designed to dive into broadband channels and to enable services like streaming video or sending text messages to smartphones. The broadband channels are wide enough to transmit multiple signals over the same path, whereas NB-IoT exploits narrowband channels that handle fewer signals and very small amounts of data.

With fewer bits streaming into narrowband channels, devices consume less power. On average, a five-watt battery will last 10 years transmitting data according to NB-IoT instructions, though both the number of devices on the network and the coverage area will affect lifespan. The capacity of NB-IoT is about 50,000 devices.

According to the 3GPP, the most significant feature is that existing radios can be configured to support NB-IoT with a simple software upgrade. At least 12 major wireless carriers, equipment makers, and chipmakers—from AT&T and China Mobile to Ericsson and Qualcomm—are already testing NB-IoT.

The industry was only slightly divided over the standard's operation. Wireless carriers and chipmakers lined up behind two major proposals: the first was called Narrowband LTE and found support among Ericsson, Intel, Nokia, and Verizon. Huawei and China Unicom backed the rival standard, also known as Narrowband Cellular IoT (CIoT).

After the proposals were submitted last September, the 3GPP wasted little time. According to Dino Fiore, the chairman of the 3GPP, it took only nine months to render down the proposals and write NB-IoT into the latest version of LTE, also known as Release 13. The new standard is now "frozen" and only minor

changes will be considered, he said.

NB-IoT is not the only cellular standard to be completed this year. The second is called Cat-M1, an evolution of an earlier standard known simply as Cat-1. The standard thinned out its channels and data rate by eschewing support for voice and mobile devices. Sending a single megabit per second over 1.4-MHz channels, Cat-M1 is meant to connect machines, like tiny sensors that monitor everything from industrial equipment to parking spaces in a garage.

NB-IoT emphasizes many of the same qualities. To limit power requirements, both standards allow devices to communicate with cell stations on how often to wake up and listen for signals. Unlike its close relative, it is severely economical, with data rates of 10 kilobits per second over 200 kHz narrowband channels. NB-IoT also contains support for mobile applications, such as thermal sensors in a refrigerated truck to monitor frozen fish.

The threat from other low-power networks—including new versions of Wi-Fi and Bluetooth, along with proprietary networks from LoRa and Sigfox—will likely result in a prolonged battle with NB-IoT. But some analysts think that the new cellular standards will share the airwaves with other networks rather than replace them.

NB-IoT has the benefit of a "high link budget for maximum coverage extension, low cost, and ability to reuse existing LTE networks with carrier grade reliability and security," said Nick Marshall, an analyst with ABI Research. But it might also be overkill for certain IoT devices with lighter workloads, like electronic tags or sensors embedded in parking garage spaces.

Others predict that NB-IoT will become the dominant force in the Internet of Things. "NB-IoT will crush Sigfox and LoRa because it means there will be no need for them," Matt Beal, Vodafone's director of innovation and architecture, said in a recent interview with communications news site Light Reading.

Several chipmakers are already using NB-IoT. In February, Sequans said that it was working on its chipset (called Monarch) for both standards. And earlier this month, uBlox said that it would release the first NB-IoT module toward the end of this year. ■

FACEBOOK'S TINY CELL STATION

(continued from p. 21)

their networks, Facebook might be able to reach new users of its internet service.

Other companies have found ways to extend connectivity to the backcountry. Huawei, for instance, has declined to join the Facebook project, electing instead to support its WTTx system, which creates the equivalent of a wireless fiber optic cable and works with low-cost equipment. In 2014, Nokia Networks developed an early precursor to OpenCellular, referred to as a network-in-a-box.

The question for Facebook is whether wireless carriers will sell users proprietary equipment or an OpenCellular device.

Facebook is not immune from the problem of making long-range links to the internet. OpenCellular still needs a power source and a fiber optic connection. But Facebook has been working separately on wireless backhaul, using an antenna array it calls ARIES.

Facebook planned for average people, and not an engineer, to install OpenCellular terminals. The device is small enough that someone can easily bolt it onto a telephone pole or building. It will also have an open-source operating system that can monitor and run the system remotely if technical experts are not available.

"The hardware was designed with simplicity in mind, to encourage people to deploy their own cellular networks," said Ali. "Many people might not realize that running their own cellular networks is not only possible, but also doesn't require substantial technical expertise."

Facebook has been testing OpenCellular in its laboratory. The company's engineers were able to send and receive SMS messages, make voice calls, and support basic connectivity using 2G service. The company

SAMSUNG MAKES STRIDES

(continued from p. 20)

before being absorbed by the atmosphere or blocked by walls, urban networks will have to be built with thousands of small cells on walls and utility poles. The small cells, which will blanket areas with coverage, will require tiny antenna components.

In addition, because of the high throughput of 5G networks, power amplifiers inside small cells and mobile devices must be extremely efficient, in order to keep the cost of signal processing low. Power amplifiers are the main source of power consumption in radios.

Over the last few years, making smaller and more efficient parts has taken a back seat to refining how 5G will ride the airwaves. Wireless companies are still ironing out the standard, which will not be completed until around 2019.

The result is that most equipment for diving into 5G networks is bulky and unwieldy, in stark contrast to the small devices and small cells that are rapidly forming the backbone of 5G networks. Increasingly, wireless companies are concerned that not being able to make smaller parts could delay actual 5G service to mobile users. 5G could be deployed as early as 2020.

Chipmakers and wireless equipment makers are trying to prevent what happened with 4G LTE wireless technology. The first networks were installed in Europe in 2009, but the first devices to access these networks were wireless modems, not smartphones, which did not arrive until 2011. That was another year after 4G LTE became available in the United States.

"Up until now, trial equipment has been fairly large, including the cabinet-sized base stations and user devices that must be mounted on the top of a vehicle [for testing]," said Cheun. Last month, for example, Samsung tested small-cell handovers with user equipment bolted on top of a sport utility vehicle.

The new parts are the latest sign that companies are starting to work on more than the air interface. In February, for example, Ericsson revealed its first prototype cell station for 5G networks. The entire station was small enough to be carried around like a briefcase. Only a month before, however, the wireless equipment maker carted around a cabinet-sized version on an electric scooter.

Similar efforts to shrink parts could take shape once the 3G Partnership Project starts accepting proposals on the air interface in 2017. At that point, wireless companies could concentrate more on hardware, so that the air interface is not released before chips are available. ■

2 GHz Clock Generator

- ***Square wave clocks from DC to 2.05 GHz***
- ***Random jitter <1 ps (rms)***
- ***80 ps rise and fall times***
- ***16-digit frequency resolution***
- ***CMOS, LVDS, ECL, PECL, RS-485***
- ***Phase adjustment & time modulation***

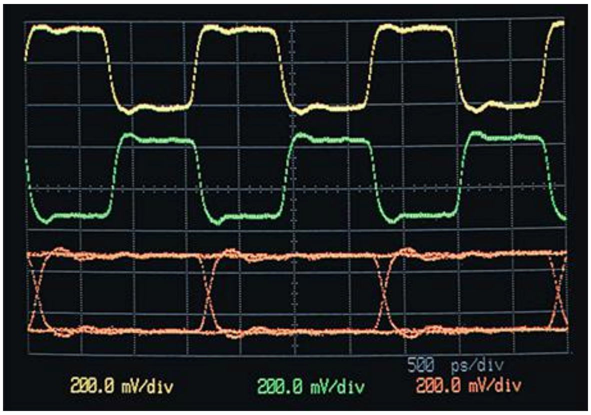

Plot shows complementary clocks and PRBS (opt. 01) outputs at 622.08 Mb/s with LVDS levels. Traces have transition times of 80 ps and jitter less than 1 ps (rms).

The CG635 generates clock signals—flawlessly. The clock signals are fast, clean and accurate, and can be set to standard logic levels.

How fast? Frequency to 2.05 GHz with rise and fall times as short as 80 ps.

How clean? Jitter is less than 1 ps and phase noise is better than –90 dBc/Hz (100 Hz offset) at 622.08 MHz.

How accurate? Using the optional rubidium timebase, aging is better than 0.0005 ppm/yr, and temperature stability is better than 0.0001 ppm.

You would expect an instrument this good to be expensive, but it isn't. You no longer have to buy an rf synthesizer to generate clock signals. The CG635 does the job better—at a fraction of the cost.

SRS

Stanford Research Systems

Phone: (408)744-9040 • info@thinkSRS.com • **www.thinkSRS.com**

Inside TRACK with Ken Karnofsky,

Senior Strategist, Signal Processing, MathWorks

Interview by CHRIS DEMARTINO, Technology Editor

KEN KARNOFSKY is senior strategist for signal processing applications at MathWorks. Throughout his 20-year career—first with BBN Technologies, and then with MathWorks—Karnofsky has been involved in the development and marketing of software for signal processing and data analysis technologies. He holds a bachelor's degree in systems engineering from the University of Pennsylvania.

"The changes in RF technology are driving a need for several improvements in modeling and simulation software."

CD: How has MathWorks adapted to meet the needs of today's RF engineers?

KK: Today's RF engineers have very different needs, because today's RF devices and radios integrate RF and digital technologies to a degree never seen before. Emerging approaches for 5G design include hybrid RF and digital signal processing (DSP) techniques that require even more highly integrated technology. As a result, RF engineers—as well as system and digital engineers, for that matter—need to understand how the RF front end affects system performance and how to partition designs between RF/analog and digital components.

The enhancements to our MATLAB and Simulink platforms integrate highly accurate RF and antenna modeling with advanced DSP algorithm design and implementation. This enables more effective collaboration among RF, digital, and system engineers to allow for faster development cycles and more thorough design verification.

CD: How have modeling and simulation software requirements changed in comparison to five or 10 years ago?

KK: The changes in RF technology are driving a need for several improvements in modeling and simulation software:

1. Improved integration of RF, antenna, and digital modeling and simulation.

2. Faster simulation of complex RF architectures to facilitate rapid design exploration.

3. Connectivity to a range of software-defined radio (SDR) and RF test hardware to accelerate and lower the cost of prototyping and design verification.

CD: How can design teams that consist of engineers who specialize in various disciplines work

together to create more efficient solutions?

KK: Design teams can use software that enables them to model and simulate digital and RF components in the same environment, at multiple levels of fidelity. This enables system engineers to quickly build a reference design, and for each design team to elaborate the design with high-fidelity behavioral models that incorporate DSP, RF, antenna, mixed-signal, and control models. System-level simulation using these models provides insight into component interactions, exposes integration issues before building hardware, and enables more rigorous system verification much earlier in the development process.

CD: What are some of the challenges associated with modeling the latest wireless systems?

KK: Developing wireless systems today requires multiple design skills, including system architecture, DSP, RF, antenna, mixed-signal, digital hardware, and embedded software. Most teams don't have expertise in all those areas. Even when they do, each specialist typically uses their favored tool. This makes system integration increasingly difficult, and pushes discovery of critical problems to the end of the development process when they're most expensive to fix.

This challenge has different impacts at different stages of development. For example, researchers can't effectively explore 5G hybrid beamforming techniques when they use different tools for digital and RF design. Advanced technology teams can't prove their concepts in hardware prototypes when they have to rely on other teams for RTL implementation. And design teams are spending far too much time debugging highly integrated radio designs in the hardware lab or in the field.

CD: What are the benefits of a complete (i.e., algorithm-to-antenna) simulation?

KK: System-level (algorithm-to-antenna) modeling and simulation pay large benefits in several ways. First, simulation can eliminate many system-level and integration errors before building hardware. This is the first step in model-based design where system models automatically generate code for hardware and software implementation of algorithms, enabling algorithm designers to prototype on hardware without having to find programmers or HDL engineers from other teams. The models also provide a reusable test bench throughout the development process, saving time and ensuring consistency of testing. These combined capabilities enable faster design iterations and streamline verification. An upfront investment in modeling has been proven to reduce overall development time by 30% or more.

> **"Current [aerospace and defense] applications are driving the adoption of highly integrated RF front ends and adaptive radio technologies."**

CD: How have aerospace and defense applications changed in recent years, and how has that affected simulation requirements?

KK: Current applications are driving the adoption of highly integrated RF front ends and adaptive radio technologies. These include development of robust tactical radios and networks, interference and spectrum management, electronic countermeasures, satellite and space systems, and signal intelligence.

Defense electronics and military system designers use commercial wireless standards in a variety of ways. Researchers want to anticipate the impact of emerging technologies such as mm-wave and massive multiple-input, multiple-output (MIMO) systems. System designers are looking to adapt those standards to lower cost and improve reliability of military communications systems. Other engineers are concerned with minimizing interference from other operational systems in a shared spectrum environment. And the signal intelligence community needs to understand how to extract information from systems using these standards.

These tasks are complicated by the scope and rapid change of commercial wireless standards. Defense system designers are users of these standards; they can't afford to maintain comprehensive knowledge or in-house tools to keep up with them.

Low-cost, highly capable SDR technology is driving innovation and broader adoption. COTS SDR hardware can be connected to a PC to create highly capable testing and prototyping systems. The challenge is that those first-generation SDR tools limited even broader adoption of the technology by forcing engineers to maintain low-level programming environments, or use software tools that work only with a single vendor's hardware.

CD: What additional challenges do you think 5G technology will create when it comes to modeling and simulation?

KK: The technologies being developed for 5G such as massive MIMO, mm-wave, and new modulation schemes require innovative combinations of new baseband technologies and RF architectures. These technologies only deepen and accelerate the need for highly integrated design environments and flexible connectivity to prototyping and test hardware.

CD: In the future, how will the Internet of Things (IoT) impact design software needs?

KK: Today, most IoT designers purchase RF modules to add wireless connectivity to their products. If something goes wrong, they face a lot of time in the lab debugging a design they didn't create. Designers can instead use model-based design to simulate the integration of RF front ends into their designs, which helps them identify and fix issues earlier and at lower cost. mw

MCL B 744
ADP-2-10
MCL QBA-12
071838
MCL BP2C

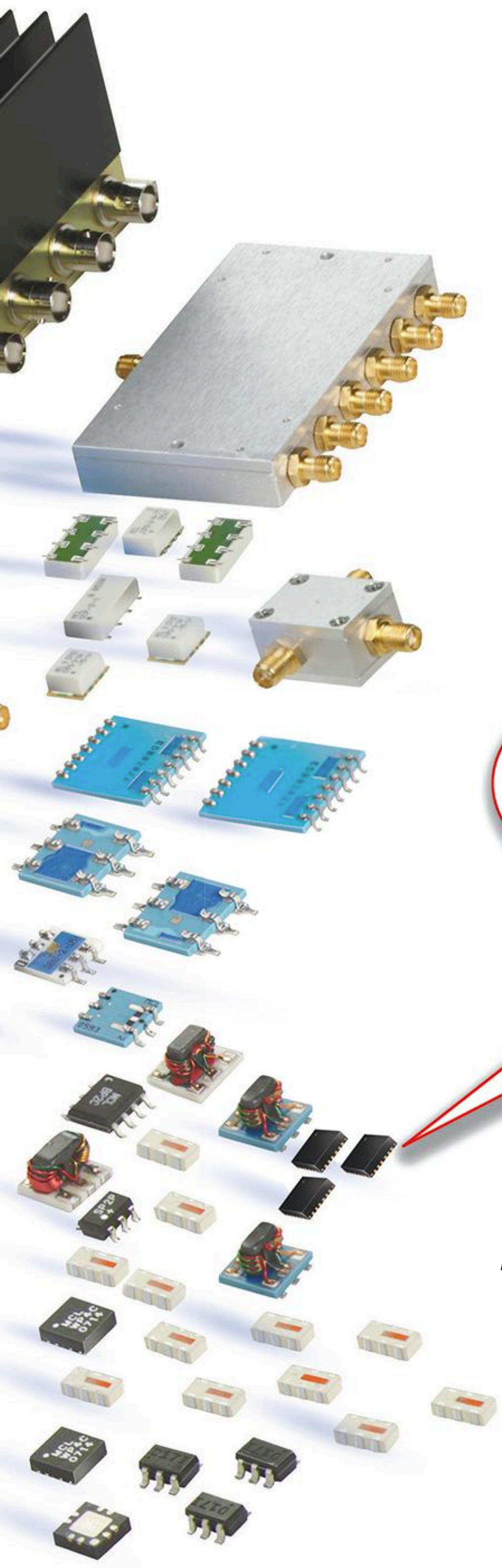

ANTENNA ARRAY AIDS ENERGY HARVESTING

ENERGY HARVESTING PLAYS an important role in gaining higher efficiency for future electronic devices, such as mobile communications equipment and IoT sensors. In search of energy-harvesting solutions, a trio of researchers from Ricoh Innovations Corp. proposed an antenna for the purpose of mechanical beamsteering to efficiently capture available RF energy.

By changing the main beam's direction, maximum power can be harvested without physically rotating the antenna to get 360-deg. coverage. Their 2 × 2 beamsteered phased-array antenna is tuned by mechanically shifting the position of the feed point, providing a continuous beamsteering angle of ±35 deg in the E-plane.

The phased-array antenna array is designed for use at S-band, at 2.4 GHz. At that frequency, the size of the array is 0.96 × 0.96 × 0.056 λ. The array features small microstrip patch antenna elements with 19.5% bandwidth. Elements include a U-shaped slot. They are fabricated on RO3010 circuit laminate from Rogers Corp., with a relative dielectric constant of 10.2. The array consists of multiple antenna elements, a feed network panel, and a movable feed structure.

Through simulations, the researchers discovered the optimum center-to-center spacing of the antenna elements for a given space to minimize mutual coupling and maximize gain. By mechanically changing the position of the feeding point, continuous E-plane steering can be accomplished without phase shifters and with low cost for the antenna array.

See "A Mechanically Beam-Steered Phased Array Antenna for Power Harvesting Applications," *IEEE Antennas & Propagation Magazine*, Vol. 58, No. 3, June 2016, p. 58.

GaAs/AlGaAs CHIP "SEES" THz WAVES

TERAHERTZ (THZ) RADIATION continues to exhibit its value and versatility in medical applications, such as focused treatment of malignant cells. THz techniques are also showing great promise in the area of materials research at the subwavelength electromagnetic (EM) radiation regions, with resolution on the nanometer scale.

In fact, a researcher from the Tokyo Institute of Technology revealed work on cryogenic THz-emission near-field imaging for close scrutiny of semiconductor devices. The research has provided invaluable information on the spatial distribution of electrons injected from an electrode into a semiconductor channel.

The new THz imaging method collects visualization data by scanning an evanescently coupled THz detector closely across a sample surface, compared to existing methods that work in illumination mode. Based on a GaAs/AlGaAs heterostructure chip, the new approach is simpler.

The GaAs chip's aperture and near-field probe are insulated by a 50-nm-thick silicon-dioxide (SiO_2) layer. It has a two-dimensional electron gas-layer heterointerface; this layer features electron mobility of 5000 cm^2/V-s. Located 60 nm below the surface of the chip, this two-dimensional gas layer acts as a THz detector. Source and drain electrodes extend to the side surfaces of the chip for electrical connections. Detected THz signals are provided as changes in voltage as a function of THz irradiation by the two-dimensional electron gas detector.

Testing and simulations revealed that chips without probes failed to detect THz signals; those with probes successfully detected THz radiation, regardless of wavelength. The spatial resolution of the near-field THz imager was found to be 9 μm.

See "Chip-Based Near-Field Terahertz Microscopy," *IEEE Transactions on Terahertz Science and Technology*," Vol. 6, No. 3, May 2016, p. 356.

RECEIVING SYSTEM CONVERTS RF TO DC

CHANGING ENERGY FROM one form to another, such as solar radiation from sunlight to dc voltage, can help meet the growing global demands for energy. It is also a practical way to provide power for remote sensors and other devices that must be "set and forget" as part of IoT applications. Even in standby mode, they consume energy and require a power source.

With this in mind, French researchers sought an alternative to a single omnidirectional antenna for collecting the RF energy in a room. They developed a system that combines six parasitic element antennas and RF-to-dc converter circuits to transform RF energy into dc voltage.

Given the growing number of wireless devices connected to a small cell, base station, or Wi-Fi gateway, the amount of "discarded" RF/microwave EM radiation is enormous and available for scavenging and reuse. Many RF-to-dc conversion circuits have been developed for this purpose, but are hampered by the limited efficiency of their antennas, or "rectennas."

The researchers boosted the efficiency of an RF-to-dc home-automation system by improving the performance of an array of six rectennas within a room. They took a cellular approach to energy harvesting within the room, combining PCB rectennas with RF-to-dc-conversion circuits on the same circuit board.

Developed for use at 2.45 GHz, the compact system provided enough energy to maintain additional circuits, such as an RF switch. Simulations showed that the system would deliver different amounts of energy based on room size; for example, 1723 and 880 mV, respectively, for rooms measuring 5 × 5 m and 10 × 10 m.

See "Multidirectional Receiving System for RF to dc Conversion Signal," *IEEE Antennas & Propagation Magazine*, Vol. 58, No. 3, June 2016, p. 22.

AMPLIFIERS HEIGHTEN PERFORMANCE to Satisfy the Next Wave

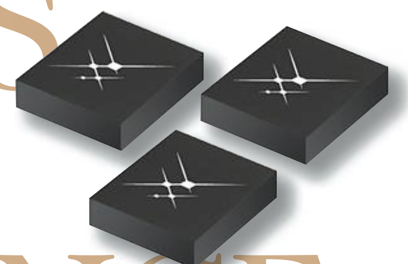

Market trends, such as small-cell infrastructure and broadband applications, are driving suppliers to deliver amplifiers with cutting-edge performance.

The pressing needs of today's applications are prompting amplifier suppliers to deliver new products to meet current high-frequency demands. One specific area that is now driving a significant amount of product development is small-cell infrastructure, which is a growing market. As many turn to small cells to drive wireless networks, amplifier suppliers are launching new products in support of this need.

Small-cell infrastructure is certainly not the only area that must be addressed by suppliers. Applications demanding wideband frequency performance have prompted the launch of several new broadband amplifiers. Such amplifiers can enable both commercial and military applications that require broadband performance.

AMPLIFIERS FOR SMALL CELLS

Small cells function as miniature base stations, enabling wireless capacity to be enhanced. They can be utilized in both indoor and outdoor locations to meet wireless traffic demands. Of course, small-cell infrastructure requires the proper components, such as amplifiers.

One company supporting the fast growing small-cell market is Skyworks (www.skyworksinc.com). "As mobile devices and applications supporting the Internet of Things (IoT) proliferate, there is an immediate and substantial increase in network load," says David Stasey, the company's vice president and general manager of diversified analog solutions. "An unprecedented deployment of small-cell systems is helping improve network performance."

1. These power amplifiers (above) are intended for small-cell base stations. *(Courtesy of Skyworks)*

Skyworks recently introduced the SKY66184-11, SKY66185-11, and SKY66186-11 power amplifiers (PAs) for small-cell infrastructure *(Fig. 1)*. "Our newest amplifiers provide infrastructure original equipment manufacturers (OEMs) with an entire portfolio of solutions for next-generation global cellular networks that cover all major LTE bands," continues Stasey. "These amplifiers are compact devices designed for FDD/TDD small-cell base stations, enabling small-cell infrastructure OEMs to radically simplify their system architecture.

"These solutions feature high gain and linearity, along with the capability to operate under high temperatures (+85°C)," he adds. "The amplifiers are also pin-to-pin compatible, providing support of all 3rd Generation Partnership Program (3GPP) bands. Their superior output return loss makes them easy to use. An integrated coupler for output-power monitoring minimizes the number of external components required. Furthermore, the amplifiers operate off a single +3.3-V power supply."

The SKY66184-11 operates from 2,110 to 2,170 MHz, covering LTE bands 1, 4, and 10. The SKY66185-11 spans 851

"Small cells function as miniature base stations, enabling wireless capacity to be enhanced. They can be utilized in both indoor and outdoor locations to meet wireless traffic demands. Of course, small-cell infrastructure requires the proper components, such as amplifiers."

to 894 MHz, which covers LTE bands 5, 6, 18, 19, 26, and 27. The SKY66186-11, which covers a frequency range of 728 to 768 MHz, is intended for LTE bands 12, 13, 14, and 17. In addition, active biasing circuitry is integrated in these PAs to compensate performance over temperature, voltage, and process variation. Each device can provide +23 dBm of output power with an adjacent-channel leakage ratio (ACLR) of −50 dBc at +85°C.

Other companies that are enabling small-cell infrastructure include Qorvo (www.qorvo.com), which recently announced a new line of PAs that target small-cell base stations. The product line contains eight new PAs, covering frequencies that range from 1,805 to 2,400 MHz. The TQP9218 and TQP9418 PAs both operate from 1,805 to 1,880 MHz. A frequency range of 1,930 to 1,990 MHz is covered by the QPA9219 and QPA9419 PAs (the QPA9219's datasheet specifies a frequency range of 1,930 to 1,995 MHz).

2. This low-noise amplifier attains a noise figure less than 0.8 dB. *(Courtesy of Guerrilla RF)*

Furthermore, the TQP9221 PA spans 2,010 to 2,200 MHz, while the TQP9421 PA covers 2,110 to 2,170 MHz. Finally, the TQP9224 and TQP9424 PAs both operate from 2,300 to 2,400 MHz. The TQP9218, QPA9219, TQP9221, and TQP9224 PAs are rated as 0.25-W amplifiers, while the TQP9418, QPA9419, TQP9421, and TQP9424 PAs are specified to deliver 0.5 W of output power.

PAs are obviously not the only components required for small-cell infrastructure: Low-noise amplifiers (LNAs) are crucial components as well. One recently introduced product is the GRF2105 LNA *(Fig. 2)* from Guerrilla RF (www.guerrilla-rf.com). With its broadband performance, the GRF2105 is targeted at the small-cell market. This LNA, which is housed in a 1.5- × 1.5- × 0.5-mm, 6-pin dual-flat-no-lead (DFN) package, delivers greater than 20.5 dB of gain at frequencies as high as 2,700 MHz and approximately 19 dB of gain at 3.8 GHz. Furthermore, the GRF2105 has a noise figure below 0.8 dB at 2,500 MHz.

BROADBAND PERFORMANCE

Recently, several broadband amplifiers have been unveiled to satisfy wideband frequency requirements. One company focused on delivering broadband performance is Custom MMIC (www.custommmic.com). "With new and ever-increasing demands of the internet and multimedia on the commercial side, as well as broadband high-data-rate communications and electronic-warfare (EW) links on the aerospace and military side, RF/microwave amplifiers are being used in many broadband applications," says Jim Moniz, a principal engineer at the firm. "We have developed multiple wideband BroadRange distributed amplifiers, covering dc to 22 GHz with a unique positive gain slope."

Moniz adds, "Unlike most distributed amplifiers, our amplifiers—such as the CMD192, CMD240, and CMD241—have positive gain slope with increasing frequency. This performance compensates for the higher-frequency losses that are typical of other components in a system. In addition to the positive gain slope, these designs include the use of on-chip tracking circuits to ensure consistent performance over temperature and process variation."

System designers can greatly benefit from the positive gain slope provided by these amplifiers, as it enables components (such as gain equalizers) to be removed from the overall system design. Moniz explains, "The positive gain slope of the amplifier allows broadband system designers to eliminate equalizers or added amplifiers, which are used to compensate for the typical negative gain slope of most wideband components with increasing frequency."

The recently launched broadband amplifiers from Custom MMIC include the aforementioned CMD240 and CMD241 BroadRange models. The CMD240 operates from dc to 22 GHz, while the CMD241 spans 2 to 22 GHz. The CMD238 wideband amplifier, which covers 2 to 20 GHz, was also recently unveiled.

Finally, among the latest products from Mini-Circuits (www.mini-circuits.com) is the LVA-123+ wideband amplifier, which covers a frequency range of 0.01 to 12 GHz. Delivering 17.3 dB of gain at 2 GHz, the LVA-123+ has a gain flatness of only ±0.6 dB from 0.05 to 6 GHz. The amplifier is well-suited for a number of applications, including base-station infrastructure, test instrumentation, satellite communications (satcom), and more.

To summarize, one can see that small-cell infrastructure will continue to be a focal point in the coming days ahead. And broadband requirements are driving suppliers to offer amplifiers with wideband performance. These and many other requirements will surely keep companies busy for quite some time. mw


YOUR COMPLETE MILLIMETER WAVE
SOLUTION
new
Low-Cost
VNA Extender
MANY ITEMS IN STOCK
MADE IN USA
www.sagemillimeter.com | 3043 Kashiwa Street, Torrance, CA 90505
T: 424-757-0168 | F: 424-757-0188 | sales@sagemillimeter.com
SAGE
Millimeter, Inc.

JACK BROWNE | Technical Contributor

Accuracy is Vital When Testing Material Qualities

Dielectric constant and dissipation factor are among the essential material parameters used by circuit designers, and they must be measured precisely for accurate models.

CIRCUIT MATERIALS like those based on polymers and resins serve as foundations for high-frequency circuits. They are characterized by various parameters that describe electrical and mechanical properties, such as the complex permittivity (the real part of which is the dielectric constant) and complex permeability (which also has imaginary and real parts that can be used to find a material's loss tangent or dissipation factor).

Proven measurement methods are crucial for ensuring accurate results of material measurements and for making valid comparisons of material parameters from different suppliers. Knowing which test methods were applied and at which frequencies can also ensure that proper material parameter input data is supplied to a computer-aided-engineering (CAE) software simulator used as part of the circuit-design process.

Many of the measurement methods developed for permittivity and permeability use calculations based on scattering (S) parameter measurements of a material sample with a microwave vector network analyzer (VNA). Different test methods have been adopted by various material manufacturers and technical organizations. In fact, the IPC (www.ipc.org) offers 13 different test methods for determining dielectric constant and/or dissipation factor. These disparate test methods may yield different results, but there are usually reasons for those differences if the details of the test methods are understood.

Printed-circuit-board (PCB) materials for RF/microwave circuits are anisotropic in nature, meaning that some characteristics, such as dielectric constant, vary in the different axes of the material. The z-axis or thickness of a circuit material is usually of most interest, since this will serve as the dielectric layer, for example, between transmission lines and a ground plane in a microstrip circuit.

PCB materials are supplied as laminates, with copper or other conductive metals attached to the dielectric, or as prepregs, without metal backing *(Fig. 1)*. Measurements of PCB dielectric properties are performed on prepregs or laminates from which the conductive metals have been completely removed. That's because the presence of metal in the material will change the material's dielectric nature and any subsequent S-parameter measurements.

1. Circuit materials are available as prepregs and with metal backing, although the former are better suited for material parameter measurements. *(Courtesy of Rogers Corp.)*

MAKE A REFERENCE

Some material characterization methods involve fabricating a reference circuit, such as a microstrip resonator, on a material under test (MUT). By relating the resonator's physical dimensions/wavelength to theoretical values for relative permittivity (dielectric constant) and dissipation factor, it is possible to determine the relative dielectric constant and dissipation factor based on measured resonant frequency, resonator bandwidth, and electrical lengths. In such a measurement, the effects of the copper conductor are included in the dielectric-material analysis. While the approach can yield accurate results, it provides values at only one frequency rather than broadband analysis.

Another commonly referenced measurement method for PCB dielectric constant and dissipation factor, which also uses a resonant circuit, is the clamped stripline resonator test. The approach involves forming a stripline resonator in a ground-signal-ground layer configuration that is mounted in a clamping test fixture to determine the dielectric constant and dissipation factor as a function of the MUT's thickness *(Fig. 2)*.

Other methods based on measuring resonant frequencies of known structures are used to evaluate the dielectric constant and dissipation factor of a MUT in the x and y axes (length and width). These include the split-post dielectric resonator (SPDR) method, the rectangular cavity approach, and the open-cavity resonance method. In all three techniques, the electric field is perpendicular to the MUT, revealing the characteristics of the dielectric material in the x-y plane rather than in the z-direction (thickness). For many PCB materials, the value of the dielectric constant can be quite different in the x-y plane than in the z-axis due to use of materials, such as ceramic or woven glass, that serve to reinforce the polymer or resin circuit material.

LEVERAGING THE VNA

The availability of high-performance commercial microwave VNAs has put basic material parameter measurements within reach of many engineers seeking validation of their PCB datasheets. Many leading VNA makers offer application notes related to material measurements, based on test methods that convert S-parameters to material parameters.

Some of these methods are as straightforward as connecting a section of waveguide or coaxial transmission line to the VNA and inserting a small sample of the MUT within the end of the transmission line in order to perform transmission and reflection measurements. Others, such as the full-sheet-resonance (FSR) method, measure a known length of circuit board, evaluating the resonant peaks or standing waves at different frequencies to calculate the dielectric constant.

The appropriate equations can relate the S-parameter measurements of reflection and transmission to the permittivity and permeability of the MUT. Although not considered "nondestructive" measurements, which require precisely machined samples of the MUT for insertion within the waveguide or coaxial line, they can provide information about the broadband characteristics of dielectric material. Unfortunately, because such small samples are involved in the measurements, they are not applicable to determining material characteristics across a large sheet of material, such as the tolerance of the dielectric constant.

Additional material measurement techniques using a VNA include the short-circuit-line (SCL) and open-ended coaxial probe methods, both of which provide broadband values for complex permittivity and permeability.

These VNA measurement methods test for S-parameters and then solve for the material unknowns, including complex permittivity and permeability. Errors in the calculations can arise at half-wavelength multiples of the test frequency and the size of the material sample. Therefore, normal practice is to test a material sample that is less than one-half wavelength long at the highest frequency of interest.

2. This test fixture is used for dielectric measurements with a VNA when applying the clamped stripline resonator approach. *(Courtesy of Rogers Corp.)*

The various transmission-line methods based on insertion of a sample also rely on precise machining of the same to avoid the presence of air pockets between the probe or transmission-line conductor and the surface of the material sample. Any air in the sample will effectively lower the result of any calculations of dielectric constant from the measured S-parameters.

FROM COMPLEX TO SIMPLE

Some material measurements are considerably more elaborate, such as dielectric constant as a function of temperature and coefficient of thermal expansion (CTE). This measures how the different material components of PCB expand with temperature and how a PCB might react when attached to another material (e.g., a metal heat-sink). The measurement is also critical for portions of the PCB on which metal meets dielectric surfaces—for instance, plated through holes (PTHs)—since significant differences in CTEs may result in stress and reliability problems.

Some material measurement methods are quite intuitive and can be performed with fairly simple test circuits. The differential phase-length method, for example, is based on using a VNA to measure the unwrapped phase of different lengths of microstrip transmission lines formed on the material under test.

The method was clearly explained during a technical presentation by John Coonrod of Rogers Corp. during the 2013 International Microwave Symposium (IMS) in Seattle. In fact, it is available as part of a YouTube video on the company's website (www.rogerscorp.com). The firm also offers free downloadable personal-computer (PC) software to determine a material's dielectric constant from the phase measurements. mw

CHRIS DeMARTINO | Technology Editor

Test Solutions Clear the Way to Consumer-Ready IoT

Manufacturers of IoT devices must implement the proper approach when it comes to testing their products.

AS THE INTERNET OF THINGS (IoT) continues to emerge, so do demands for efficient testing of the wave of products arriving into this arena. No question, the IoT encompasses a wide range of industries that utilize various wireless technologies. Needless to say, then, that IoT device testing requirements are also great in scope.

Taking a vigilant approach when it comes to test, such as performing testing throughout the product-development cycle, can help companies developing IoT-based products avoid dreaded pitfalls. Such companies are being aided by the latest solutions coming from suppliers of test-and-measurement equipment.

For example, wireless test sets that support multiple standards can be used in high-volume manufacturing environments, offering both performance and flexibility. With the impact of IoT looming, proper testing becomes ever-more important for device manufacturers.

UNIVERSAL IoT TEST SOLUTIONS

The IoT can mean different things to different people due to its broad appeal. “If you ask 10 people what IoT means, you’re likely to get 10 different answers that range from big data to the connected car,” says Brian Davis, field applications engineer for Wireless Products, Anritsu (www.anritsu.com). “One common denominator in all IoT applications is that products must be connected via wired and/or wireless technologies.

“Most IoT solutions are projected to be relatively close range and will likely use non-cellular technologies, such as Bluetooth low energy (BLE), ZigBee, or possibly point-to-point connections envisioned in the future for 5G,” adds Davis. “Longer-range connections can be provided by cellular or low-power wide-area network (LPWAN) technologies, such as LoRa, Narrowband-IoT (NB-IoT), or 6LoWPAN.”

In terms of IoT performance requirements, several are particularly critical, such as range. Proper testing is needed to ensure that these requirements are met. “In addition to range, one key consideration when selecting the appropriate technology is the reliability requirement of the end application,” says Davis. “For example, a connected car using multiple sensors and a high data rate will require extremely reliable real-time connections. Extensive testing and quality assurance in the manufacturing phase is required in these designs.”

By utilizing a single test platform that is customizable to a user’s specific needs, Anritsu believes that IoT-based testing can be simplified. Davis explains, “Testing IoT devices

1. This platform can accommodate as many as four test modules. *(Courtesy of Anritsu)* will vary depending on the technologies chosen for the product and the reliability requirements. IoT device testing, however, does not have to be complex. Wireless IoT technologies are many, but the production testing for all of them is handled in a similar manner. This means that a larger portion of IoT device testing during production can be handled by a single solution—as long as it is a customizable testing platform that can support the most common IoT technologies. One example is our MT8870A universal wireless test set *(Fig. 1)*.

2. Litepoint's test system is able to cover frequencies to 6 GHz. (Courtesy of LitePoint)

"Solutions such as these consist of a mainframe, measurement modules, and software, allowing users to simply add or remove modules as testing needs to be changed," he continues. "In addition, the single hardware module architecture, such as in the MT8870A, supports all cellular and non-cellular technologies. If many production lines use the same test platform, it is possible to transfer measurement capacity from one line to the other just by removing and reconnecting a module. This capability makes IoT wireless device manufacturing faster and more economical."

FINDING A SUCCESSFUL IoT TEST APPROACH

Another company at the forefront of IoT testing is LitePoint (www.litepoint.com), which supports IoT test requirements with products like the IQxel-M test system *(Fig. 2)*.

"There's good and bad when it comes to RF and the IoT," says Adam Smith, director of product marketing at LitePoint. "There is an embarrassment of riches in terms of different technologies to choose from. But product designers can get overwhelmed trying to determine which technology to choose. Key considerations include operating range, throughput, number of devices supported by the protocol, industry acceptance and momentum for the protocol, etc. It is very early in this industry, which means that there are many technologies to choose from. But the downside is that product designers have to be very strategic when making their choice.

"Most IoT companies are designing their product functionality first and adding on RF capabilities later based on reference designs from chip makers," he continues. "Without testing throughout the product development cycle, this approach will not yield a high-quality user experience that is vital for IoT products."

LitePoint has actually witnessed several customers experience problems that could have been avoided if they took a different approach to testing. "Several IoT customers have come to us at the end of their product development," adds Smith. "Because they didn't think about testing at all, there are a lot of things they missed that are impacting the performance of their systems—antenna access or performance of the product in the final form factor. These missed points would have become very apparent if they had performed testing during the product design phase."

The company also believes that RF performance and functionality is now more critical than ever. "With the IoT, we're entering an era where RF performance and functionality is becoming harder to separate from the overall product functionality," says Smith. "As a result, it is even more essential to ensure that RF performs as specified.

"Consumers may invest in a wireless front-door lock to make them safer, but it won't lock," he continues. "They won't be able to determine that the lock system was great, but the RF was faulty. They will only say that the whole product didn't work. These are the kinds of quality issues that can keep IoT companies with real innovation from succeeding."

AUTOMATION TEST REFERENCE

Other companies providing IoT test solutions include Keysight Technologies (www.keysight.com), which offers an IoT automation test reference solution that consists of both hardware and software. The reference employs the E6640A EXM wireless test set along with integrated software to satisfy large-volume manufacturing requirements. The E6640A EXM supports multi-device testing, as it can have as many as four transceiver (TRX) channels.

The test reference solution takes advantage of the Signal Studio software to generate a range of standard waveforms. Users can also import their own waveforms. In terms of signal analysis, the E6640A EXM offers the test capability to support a wide range of wireless standards like Bluetooth, ZigBee, Z-Wave, and many others.

To sum it up, as the IoT gains traction, testing becomes more crucial. On that front, test-and-measurement companies have unquestionably supported the IoT by providing a range of solutions to meet its diverse needs. As the IoT moves along, device manufacturers must implement the proper test methodologies if they wish to succeed. mw

ADEL B. ABDEL-RAHMAN | Professor
Department of Electronics and Communications Engineering, E-Just-Alexandria, Egypt
Faculty of Engineering, South Valley University-Qena, Egypt; e-mail: adel_b15@yahoo.com

AHMED A. IBRAHIM | Professor
Faculty of Engineering, Minia University, Egypt;
e-mail: ahmedabdel_monem@mu.edu.eg
Institute of Micro and Sensor Systems, University of Magdeburg, 39106, Magdeburg, Germany

Metamaterial Enhances Microstrip Antenna Gain

Single and multiple layers of metamaterials formed as lenses can improve the impedance matching, gain, and fractional bandwidth of compact microstrip antennas.

High antenna gain is generally desirable for communications systems, whether terrestrial or based on satellites. The use of metamaterials in single or multiple layers has been shown to contribute a great deal to the design of a high-gain microstrip antenna at 10.5 GHz. With a double-negative electromagnetic (EM) constant, these metamaterials exhibit properties not normally found in circuit materials.

Structures formed of the metamaterials act like a lens for a microstrip antenna, boosting gain and enhancing the radiation pattern for greater coverage. These metamaterial-equipped antenna designs feature increased bandwidth (from 3.64% to 4.68%) when compared to a conventional microstrip design.

Patch antennas are often desirable for wireless communications systems for their low profile, compact size, ease of implementation, and low implementation cost. Unfortunately, patch antennas typically exhibit low gain and narrow bandwidths. Several approaches have been presented to overcome these disadvantages.[1-3] For example, arrays of several patch antennas have been used to achieve increased gain. However, this approach must overcome losses associated with the feed network and coupling between antenna elements in the array.

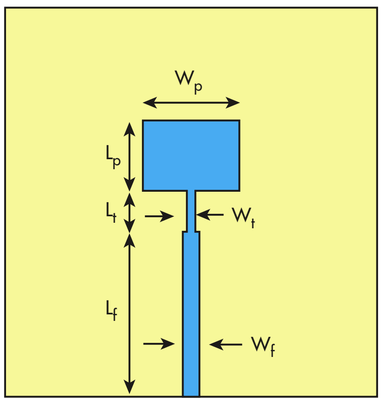

1. These are the dimensions of the microstrip antenna.

Metamaterials can provide EM properties not found in nature that can help enhance antenna gain. Left-handed materials (LHMs) were theorized in 1967 as EM plane wave propagation in a lossless medium with simultaneous negative real permittivity and permeability at a given frequency.[4] LHM is characterized by antiparallel phase and group velocities as well as nonlinear phase characteristics.[5-7] These properties have enabled the development of compact microwave components.[8-11]

The recent revival of interest in double-negative media began with Smith, Schultz, and Shelby, as inspired by the work of Pendry.[12,13] Smith demonstrated a new metamaterial that simultaneously achieved nega-

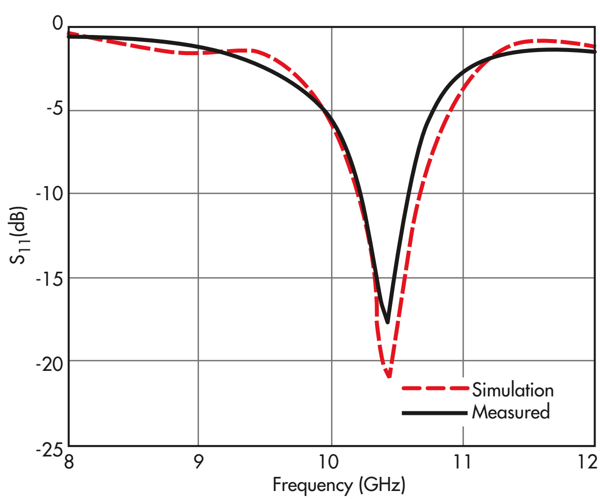

2. The plots compare the simulated and measured return loss of the microstrip antenna, designed for 10.5 GHz.

tive permittivity and permeability.[14] Different shapes of metamaterial cells have also been used to achieve double-negative characteristics.[15-21]

To better understand the benefits of using metamaterial structures with microstrip antennas, an antenna was designed with a unit-cell metamaterial lens structure; the performance of the antenna was evaluated with the Microwave Studio full-wave EM simulation software from CST (www.cst.com). *Figure 1* shows a two-dimensional (2D) layout of the microstrip antenna. It was designed on RT/duroid 5880 circuit material from Rogers Corp. (www.rogerscorp.com) with relative dielectric constant (ε_r) of 2.2 in the z-axis (thickness) at 10 GHz, dielectric loss tangent of 0.0009, and thickness of 0.787 mm.

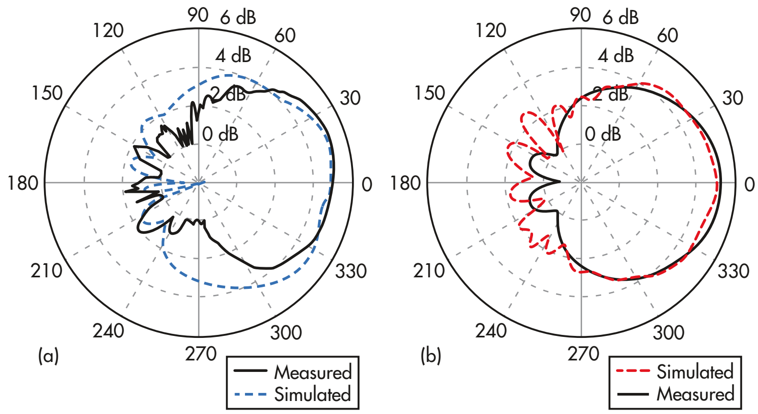

3. The radiation patterns show simulated and measured responses at 10.5 GHz in the (a) E-plane and (b) H-plane.

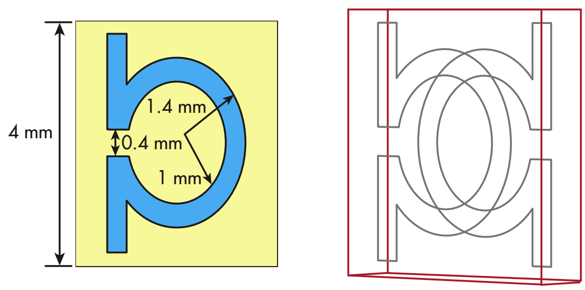

4. The dimensions of the metamaterial unit cell or lens are shown here.

The optimization of the antenna is carried out using CST Microwave Studio commercial software. The antenna measures 50 × 60 mm. 50 mm × 60 mm. The patch maintains a length, L_p, of 8.8 mm, width, W_p, of 13 mm, and thickness of 35 µm. The antenna is impedance-matched by means of a quarter-wavelength ($\lambda/4$) transformer with a length, L_t, of 5 mm and width, W_t, of 0.9 mm. The antenna is fed by means of 50-Ω microstrip line with a width, W_f, of 2 mm and length, L_f, of 20 mm.

Figure 2 compares measured and simulated values for return loss, which are in good agreement. From the simulations, it is apparent that the antenna has an impedance bandwidth from 10.30 to 10.75 GHz. However, from the measurements, the fabricated antenna exhibits an impedance bandwidth from 10.20 to 10.58 GHz, with a center frequency, f_0, of 10.43 GHz. *Figure 3* shows the antenna's simulated and measured radiation patterns, in the E and H planes at 10.5 GHz, which also agree closely. The measured gain is 5.8 dB.

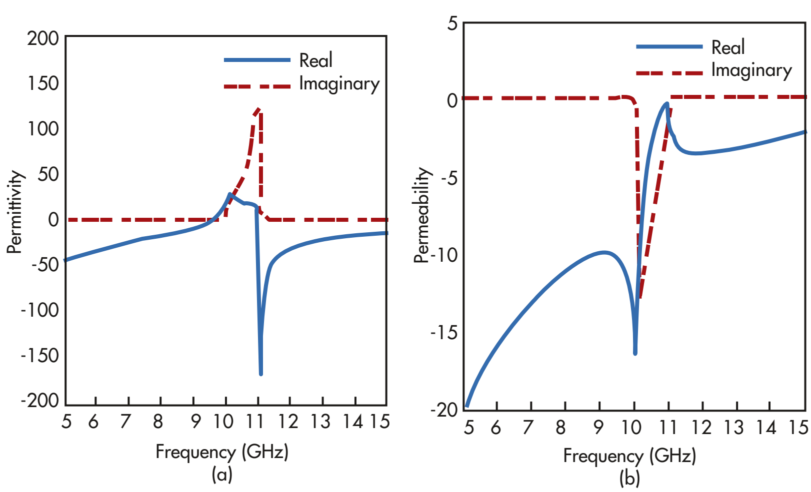

5. The plots show the real and imaginary values for the metamaterial unit cell (a) permittivity and (b) permeability.

Figure 4 presents (a) 2D and (b) three-dimensional (3D) layouts of a single metamaterial unit cell for an omega structure. In this structure, two perfect electric conductors (PECs) with thickness of t = 0.035 mm are integrated on RO4003 circuit material from Rogers Corp. with relative dielectric constant (ε_r) of 3.55, dissipation factor of 0.0027, and thickness of 0.813 mm. This structure is a complex design that couples the rod and ring.[22]

The effective permittivity and the effective permeability of the omega structure can be calculated by an approach based on extraction from the transmission and reflection characteristics of the metamaterial omega structure.[22,23] This extraction technique consists of several steps. First, the complex normalized wave impedance (z) and refractive index (n) are retrieved from the S-parameters. Second, the effective permittivity (ε_{eff}) and permeability (μ_{eff}) are computed from the n and z values. The data are calculated with the aid of the MATLAB mathematics-based simulation software from MathWorks (www.mathworks.com). *Figures 5(a) and (b)* show the effective permittivity and permeability of the omega structure.

To enhance microstrip antenna performance, it was necessary to understand the impact of the size of the omega structure serving as a lens on the radiation patterns and antenna performance. To ensure the

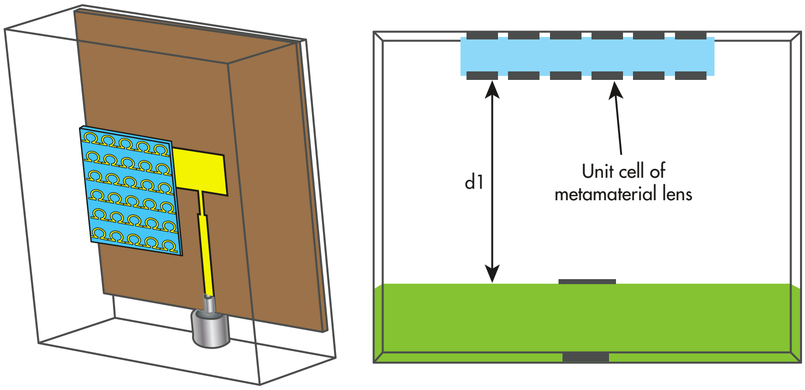

6. This is a simple layout of the microstrip antenna showing the distance to a single-layer metamaterial unit cell.

effect of the periodic structure size and to obtain the optimum return loss and radiation parameters, a parametric study on the antenna loaded with metamaterial lens at specific separation and different dimensions for the periodic structure are carried out.[24] A 6 × 5 periodic structure was considered optimal.

Figure 6 shows the antenna layout, with a single-layer metamaterial lens loaded at a distance, d1, from the patch antenna. The effect of d1 on performance was evaluated, with simulated return loss and gain for different values of d1 shown in *Figs. 7 and 8*.

When d1 equals 8 mm, at around $0.25\lambda_0$, the impedance bandwidth and gain are affected compared to the antenna without metamaterial lens, where the bandwidth and gain are less. When d1 equals 16 mm, at around $0.50\lambda_0$, the impedance bandwidth and gain are increased.

When d1 is increased to 32 mm, at around $1.0\lambda_0$, the impedance bandwidth is reduced and the operating frequency is shifted toward 10.7 GHz. The gain is reduced to 8 dB, but it is still more than a conventional antenna without metamaterial lens. For optimum performance with a single-layer metamaterial lens,

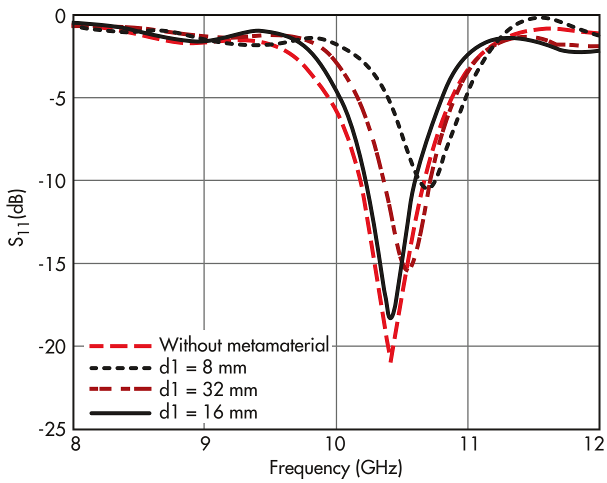

7. The plots show the simulated return loss of the microstrip antenna with a single-layer metamaterial lens at different values of distance d1.

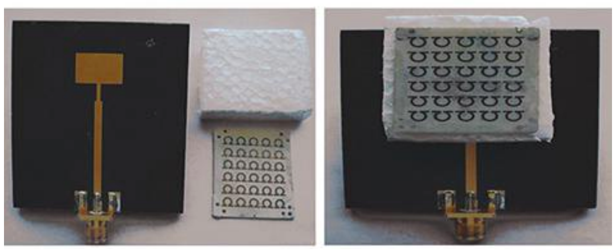

9. These photographs show different views of the fabricated antenna with a single-layer metmaterial lens.

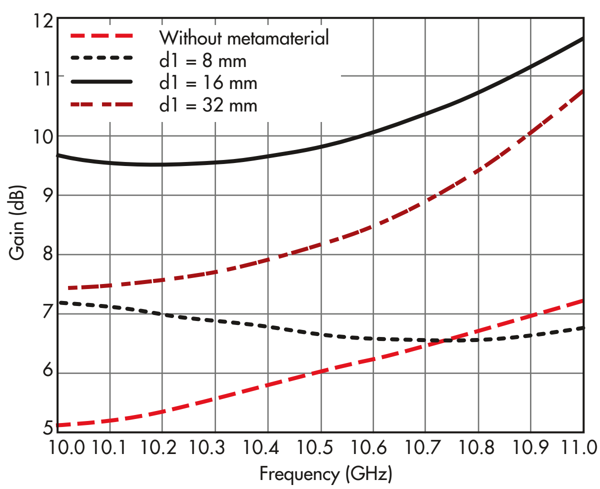

8. These plots show simulated gain for the microstrip antenna with a single-layer metamaterial lens at different values of distance d1.

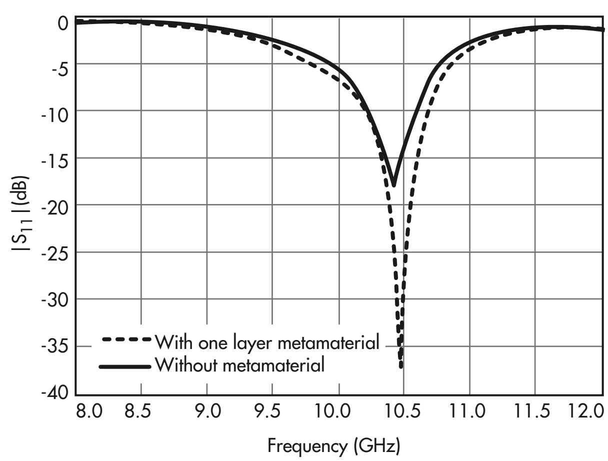

10. The return loss of the microstrip antenna was measured with and without a single-layer metamaterial lens.

d1 should be equal to 16 mm at this frequency.

To better understand the effects of the metamaterial structure, the proposed antenna was fabricated and characterized. Foam material with relative dielectric constant approximately equal to that of air (1) and thickness (d1) was added as a spacer between the metamaterial and the patch antenna *(Fig. 9)*.

Figure 10 shows measured return loss with and without the metamaterial. As can be seen, the metamaterial lens enhances the matching characteristics of the antenna. The fractional bandwidth of the antenna is increased from 3.64% to 4.68% as well. *Figure 11* shows the measured E- and H-plane radiation patterns of the antenna at 10.5 GHz.

If one metamaterial layer can help microstrip antenna performance, perhaps two layers might provide greater benefits. To explore this possibility, the effects of adding another layer of metamaterial were investigated, at a distance, d2, from the first layer above the antenna. An optimum value of d1 = 16 mm was used for the first layer. *Figure 12* shows the proposed antenna with two metamaterial layers.

The second layer was placed at different distances of $0.25\lambda_0$, $0.55\lambda_0$, and $5\lambda_0$ above the first layer, with simulated return loss and gain plotted in *Figs. 13 and 14*, respectively.

With the added metamaterial layer, the gain of the antenna increased from 5.8 to 12 dB at 10.5 GHz. It also increased from 11.8 to 12.4 dB at the lower-frequency edge of the band at 10.3 GHz and at the upper-frequency edge of the band at 10.7 GHz at a distance of d2 = 16 mm for high gain throughout the antenna bandwidth. When d2 = 32 mm, the gain of the antenna increased from 5.8 to 11.4 dB at 10.5 GHz. The optimum distances d1 and d2 for good antenna performance in the 10-GHz band were d1 = 16 mm and d2 = 16 mm. mw

For references, see the version of this article at www.mwrf.com.

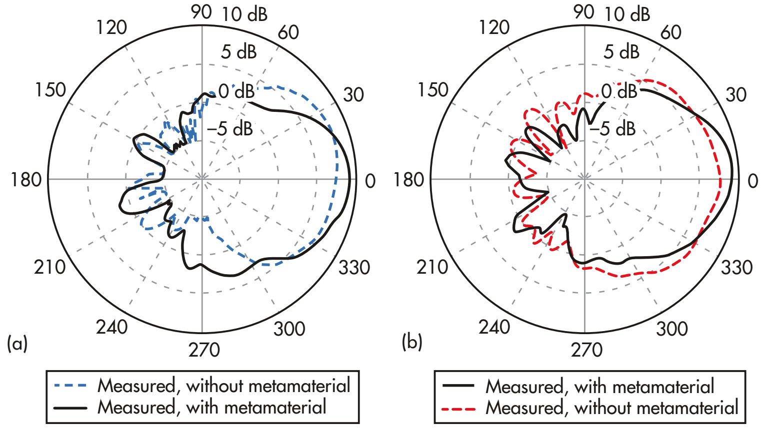

11. The gain of the microstrip antenna was at 10.5 GHz with and without metamaterials in (a) the E-plane and in (b) the H-plane.

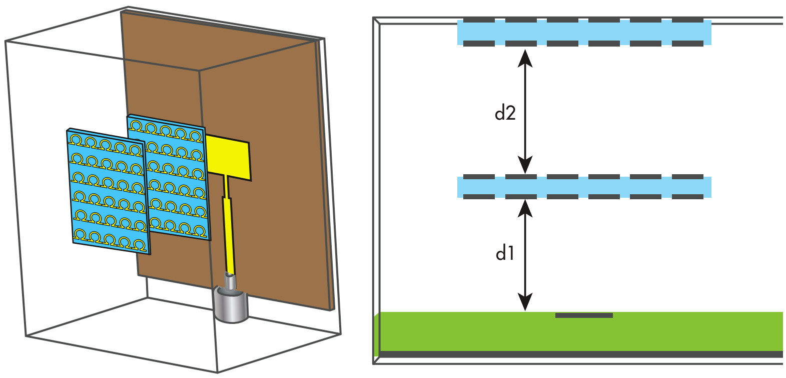

12. This layout shows the concept of the microstrip antenna with two metamaterial lenses on the left and the spacing of the lenses on the right.

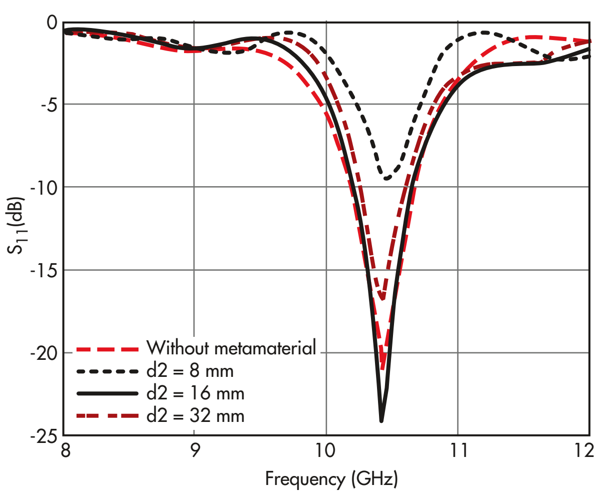

13. The antenna return loss was simulated for different values of distance d2.

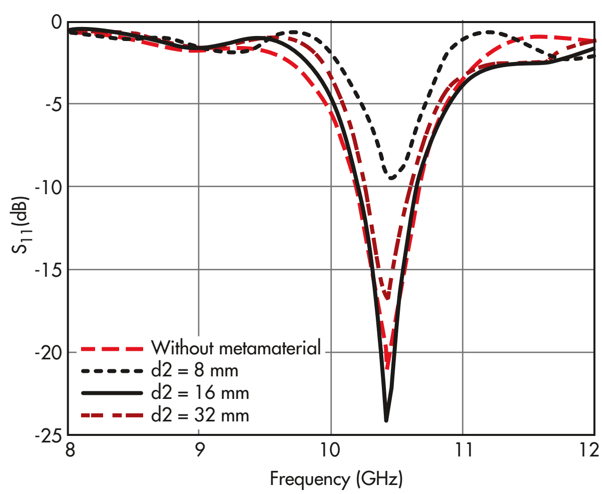

14. These plots compare the simulated gain of the microstrip antenna without a metamaterial lens and with different values of distance d2.

NASSIMA BELGACEM | Ph.D. Student
Telecommunications Laboratory of Tlemcen

MEHADJI ABRI | Doctor
Telecommunications Laboratory of Tlemcen

WAHIBA BELGACEM | Engineer
Agence Spatiale Algérienne, Oran, Algeria

HADJIRA ABRI | Doctor
STIC Laboratory of Tlemcen

Telecommunications Department, Faculty of Technology, University of Tlemcen, Tlemcen, Algeria

Flexible PIFA Antenna Serves Multiple Wireless Bands

Fabricated on flexible textile material, this planar inverted F antenna provides versatile wireless communications coverage by handling several frequency bands with a compact form factor.

Proliferation of wireless services makes an antenna capable of operation at multiple frequency bands very attractive. For that reason, a planar inverted F antenna (PIFA) was designed for wireless network applications at 1,810, 2,530, 5,260, and 5,500 MHz. A PIFA is a compact form of microstrip antenna (shaped like an inverted letter "f") that is commonly used in wireless devices, such as cellular telephones. The goal of the design efforts was to reduce the size of the PIFA antenna structure while supporting multiple applications at commonly used frequencies, including for DCS, LTE, UMTS, WiMAX, and WLAN systems.

Since modern electronic communications products typically support several wireless standards, such as third-generation (3G) or fourth-generation (4G) cellular communications and Wi-Fi, availability of a compact antenna capable of operating at multiple wireless bands can mean a significant savings in volume within the final product design. By developing an antenna covering five different radio bands, a great deal of flexibility is provided with a relative small structure. The design was simulated with commercial computer-aided-engineering (CAE) software.

Antennas for modern communications devices must support a variety of global communication standards and services. The

1. This is the geometry of the proposed multiband PIFA antenna, where L_a = 90 mm; L_b = 38 mm; L_c = 28 mm; L_d = 8 mm; L_e = 10 mm; L_f = 2.5 mm; and L_m = 23.5 mm.

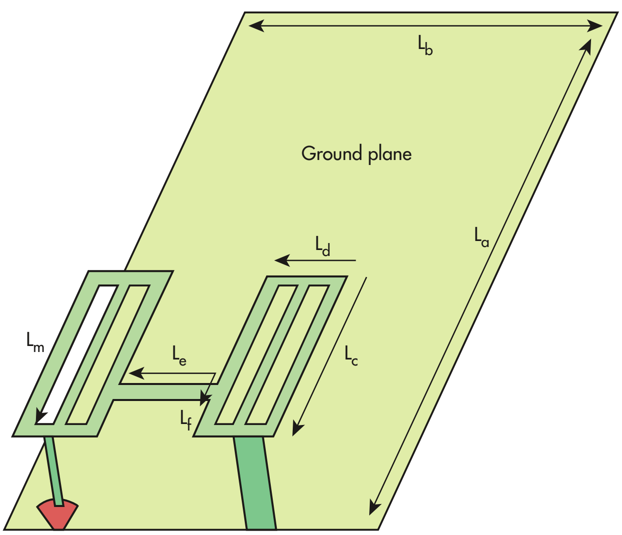

2. The plot shows the computed return loss for the multiple-band PIFA antenna.

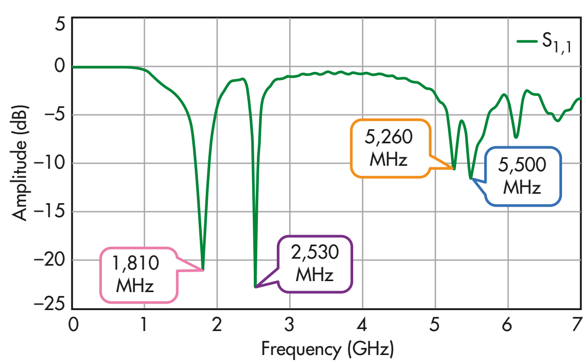

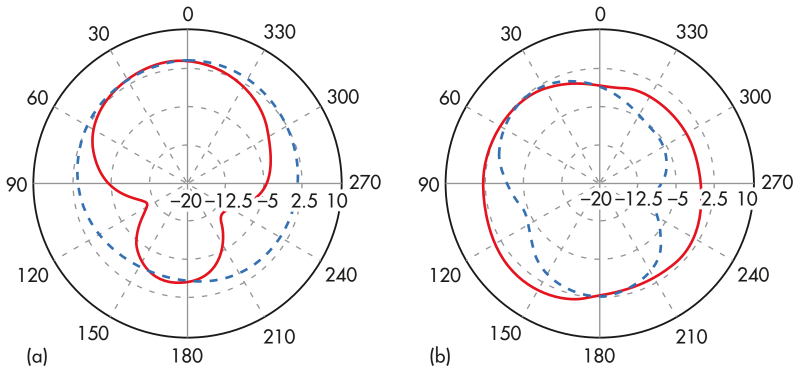

3. The polar coordinates represent the radiation patterns of the multiple-band PIFA antenna at (a) 1,810 MHz and (b) 2,530 MHz.

TABLE 1: A SUMMARY OF SIMULATION RESULTS FOR THE MULTIPLE-BAND PIFA				
Frequency (GHz)	1.81	2.53	5.26	5.50
Amplitude (dB)	–21.0	–22.7	–10.65	–11.6

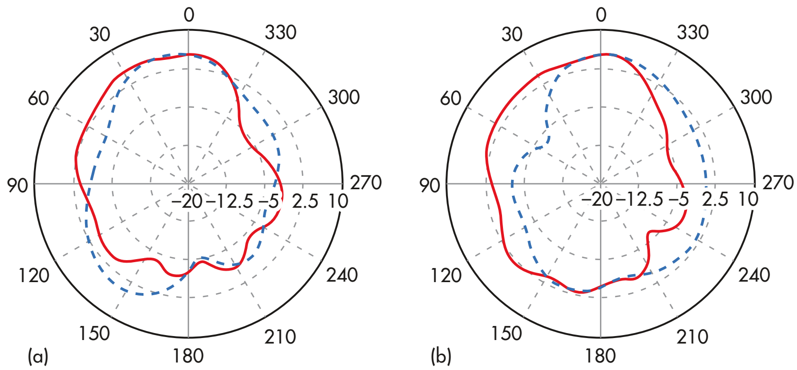

4. These polar coordinates show the radiation patterns of the PIFA antenna at (a) 5,260 MHz and (b) 5,500 MHz.

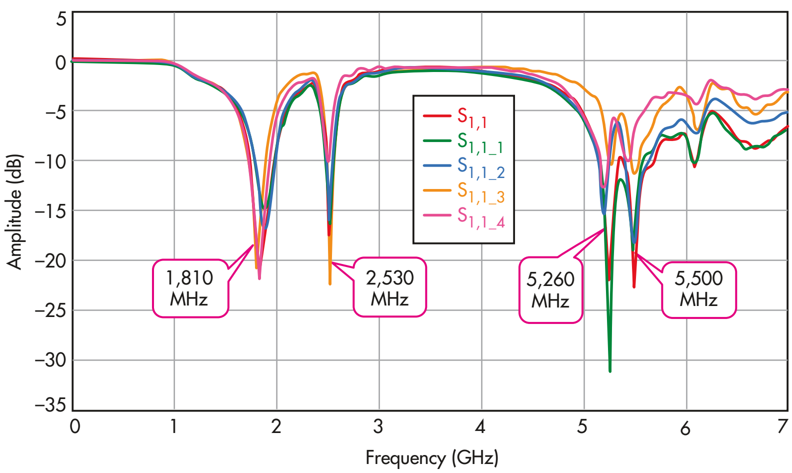

5. This is the computed return loss for the multiple-band PIFA antenna.

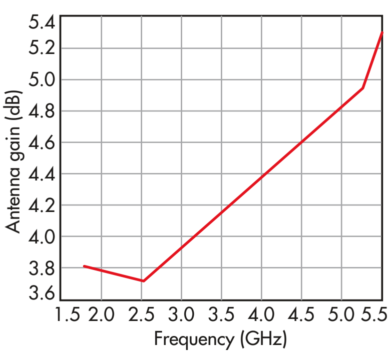

6. The plots show the simulated gain of the PIFA antenna as a function of frequency.

antennas for these modern communication devices should be capable of operating within as many bands as possible with acceptable return loss and radiation patterns in order to serve multiple cellular and noncellular communication applications. In addition to good electrical performance, the antennas should have compact, low-profile structures that are robust, lightweight, flexible, and easy to manufacture.[1-10] The rapid expansion of wireless communications has created a strong demand for antennas that are small in size and can operate across multiple wireless frequency bands to meet the requirements of modern wireless electronic devices.[2-8]

Through careful design and simulation, it was possible to develop a new PIFA covering three different wireless frequency bands: 5.26 GHz for WLANs, 2.53 GHz for Long-Term-Evolution (LTE) cellular communications, and 1.81 GHz for DCS. In spite of its multiple-band operation, the antenna achieves attractive beamwidth with good radiation efficiency in all three frequency bands.

The antenna consists of a metal ground plane with overall size of 90 × 38 × 8.05 mm and two resonators using two parallel slots in support of multiple resonant frequencies *(Fig. 1)*. A microstrip circuit connects the resonators to the ground plane.

The fundamental resonant frequency, f_r, of such an antenna structure can be found from:

$f_r = c/[4(h + L)]$

where

f_r is the fundamental resonant frequency;

c is the velocity of light in free space;

L is the length of the antenna; and

h is the height of the antenna.

The PIFA was simulated by means of Microwave Studio simulation software from Computer Simulation Technology (www.

cst.com). Simulation results were obtained for the antenna for DCS, LTE, and WLAN wireless frequency bands at resonant frequencies of 1,810, 2,530, 5,260, and 5,500 MHz *(Fig. 2 and Table 1)*.

Antenna radiation patterns are usually presented in two orthogonal planes: the E- and H-plane radiation patterns relative to the main direction of propagation. The E-plane plots show the locus of points in free space representing the radiated electric € field, while the H-plane shows the points in free space representing the radiated magnetic field (H).[1]

Figures 3(a) and (b) show the polar radiation patterns for the PIFA for frequencies of 1.81 and 2.53 GHz, respectively, with resonances within the E and H planes. It can be seen that the radiation patterns are directed along the 0 deg., 0 deg. axis for 1.81 GHz and the 180 deg., 150 deg. axis for 2.53 GHz, resulting in an omnidirectional radiation pattern.

Figures 4(a) and (b) show the polar radiation patterns for the PIFA for frequencies of 5.26 and 5.50 GHz, respectively, with resonances within the E and H planes. It can be seen that the radiation patterns are directed along the 0 deg., 30 deg. axis for 5.26 GHz and the 0 deg., 0 deg. axis for 5.50 GHz. The width of the antenna was changed to study the effects of the mechanical change *(Fig. 5)*.

Following application of the miniaturization technique, the PIFA's return loss shows improvement. The antenna design exhibited increasing gain with increasing resonance frequency *(Fig. 6)*. *Table 2* shows these gain variations vs. frequency.

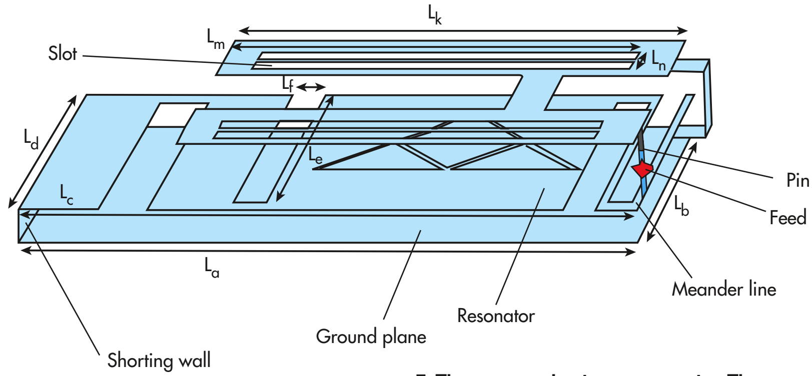

7. The proposed antenna geometry. The dimensions of the antenna are set as: L_a = 38 mm, L_b = 30 mm, L_c = 38 mm, L_d =30 mm, L_e = 28 mm, L_f = 1.5, L_m = 23.5 mm, L_n = 2 mm, L_h = 9 mm, and L_k =28.1 mm.

TABLE 2: GAIN VARIATIONS WITH FREQUENCY FOR THE MULTIPLE-BAND PIFA

Frequency (GHz)	1.81	2.53	5.26	5.50
Antenna gain (dBi)	3.80	3.71	4.94	5.28

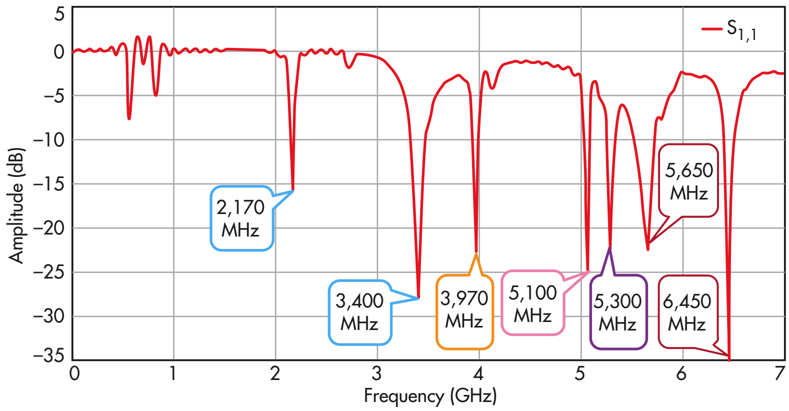

8. This is the computed return loss for the multiple-band PIFA antenna.

The antenna was implemented to cover six frequency bands with far-field radiation patterns, using meander lines and Sierpenski textile material. Such flexible antennas are suitable for body-worn antenna designs, with multiple-band coverage for the one antenna minimizing the need for additional antennas. Simulations of the flexible PIFA antenna show acceptable performance for all proposed frequency bands. The overall dimensions of the ground plane widths are 38 mm to 30 mm to 0.05 mm *(Fig. 7)*.

The authors simulated the performance of the multiple-band PIFA in six frequency bands for mobile-phone applications for UMTS (1,920 to 2,170 MHz); WiMAX (3,400 to 3,600 MHz); HiperLAN High Performance Radio LAN (HiperLAN; with frequency bands of 1,710 MHz to 2,170 MHz, as well as 4,800 to 5,800 MHz); 3G (1,885 to 2,200 MHz); and ultrawideband (UWB) applications (6500 MHz).[13]

Simulations performed with the CST software in *Figs. 8 through 10* cover dc to 7 GHz. Results show that the PIFA provides amplitude peaks in the radiation patterns at many frequencies: –16 dB for 2.17 GHz, –28 dB for 3.40 GHz, –25 dB for 5.10 GHz, –22.2 dB for

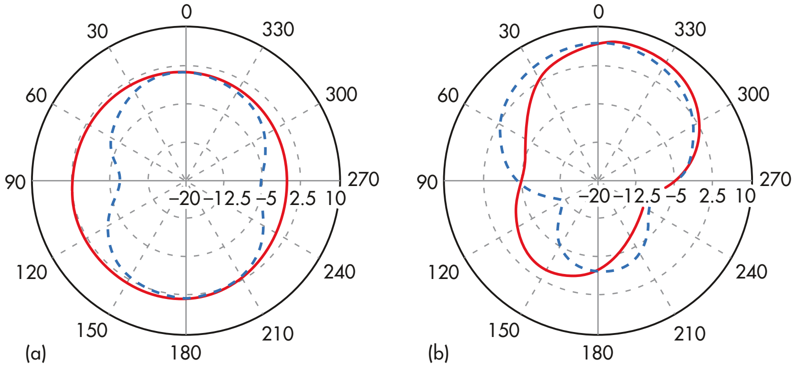

9. The polar coordinates reveal the computed antenna radiation patterns at (a) 2,170 MHz and (b) 3,400 MHz.

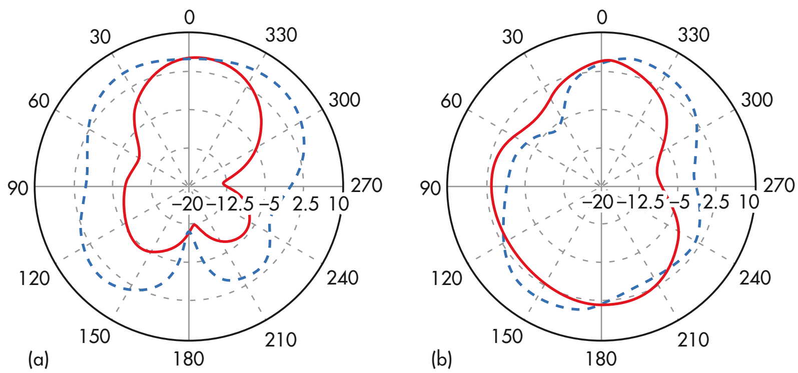

10. The polar coordinates reveal the computed antenna radiation patterns at (a) 5,100 MHz and (b) 5,300 MHz.

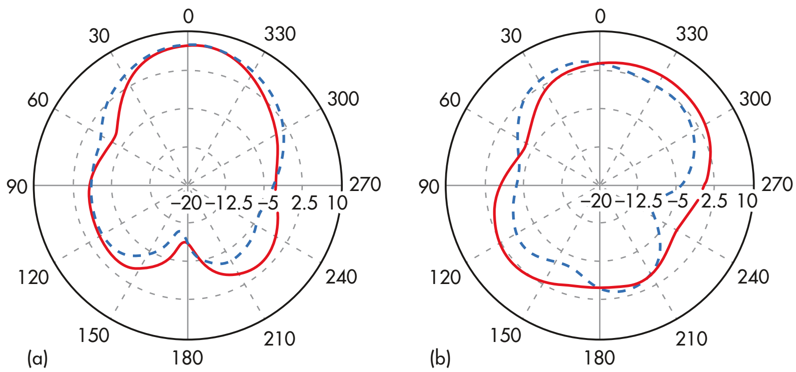

11. The polar coordinates reveal the computed antenna radiation patterns at (a) 5,650 MHz and (b) 6,450 MHz.

5.30 GHz , –22 dB for 5.65 GHz, and –35 dB for 6.45 GHz.[1]

The radiation patterns in *Figs. 9(a) and (b)* demonstrate the dependence of return loss on frequency for the PIFA. The results show the presence of resonances at the frequencies 2.17, 3.40, 5.10, 5.30, 5.65, and 6.45 GHz, with S_{11} parameter levels of –16 dB, –28 dB, –25 dB, –22.2, –22 dB, and –35 dB, respectively. Figures 9(a) and (b) show the radiation patterns in polar (E, H) coordinates for 2.17 and 3.40 GHz, with the angular degrees the patterns are directed along (180, 150 deg.) for 2.17 GHz and (0, 0 deg.) for 3.40 GHz.

Figures 10 (a) and (b) shows E- and H-plane radiation patterns in polar coordinates computed for 5.10 and 5.30 GHz, and how the E-plane and H-plane patterns move, respectively, in the 30, 30 deg. and 0, 0 deg. coordinate directions.[8]

The radiation patterns of the multiple-band PIFA change in the directions of the E and H planes for the different frequencies of operation, as shown in *Figs. 11(a) and (b)* for 5.65 and 6.45 GHz. The broadband trace in *Fig. 12* shows that antenna gain increases with increasing frequency. mw

REFERENCES

1. M. Abri, N. Belgacem, and W. Belgacem, "New GSM, DCS, and GSM/DCS PIFA Antenna Designs for Wireless Networks Applications," International Journal of Information & Network Security (IJINS), Vol. 2, No. 4, August 2013, pp. 305~310; ISSN: 2,089-3,299, 2013.
2. A.A.H. Azremi, N.A. Saidatul, R.B. Ahmad, and P.J. Soh, "Parametric Study of Broadband Planar Inverted F Antenna (PIFA) for WLAN Application," 2008 International Conference on Electronic Design, December 1-3, 2008, Penang, Malaysia.
3. L. Freytag, "Conception, Réalisation, et Caractérisation d"Antennes Pour Stations de Base des Réseaux de Télécommunication Sans Fil," Thèse de doctorat université de Limoges, Limoges, France, Novembre 2004.
4. Y. Yuan, X. Wang, X. Chen, and Y. Jun sheng, "Novel Diversity/MIMO PIFA Antenna With Broadband Circular Polarization for Multimode Satellite Navigation," IEEE Antennas and Wireless Propagation Letters, Vol. 11, 2012, pp. 65-68.
5. G.K. H. Lui and R.D. Murch, "Compact dual-frequency PIFA design using LC resonators," IEEE Transactions on Antennas & Propagation, Vol. 49, No. 7, July 2001, pp. 1,016-1,019.
6. N. Behdad and K. Sarabandi, "A varactor-tuned dual-band slot antenna," IEEE Transactions on Antennas & Propagation, Vol. 54, No. 2, February 2006, pp. 401-408.
7. K.-L. Wong, W.-Y. Chen, and T-W. Kang, "On-board printed coupled-fed loop antenna in close proximity to the surroung ground plane for penta-band WWAN mobile phone," IEEE Transactions on Antennas & Propagation, Vol. 59, No. 3, March 2011, pp. 751-757.
8. H. Morishita, Y. Kim, and K. Fujimoto, "Design concept of antennas for small mobile terminals and the future perspective," IEEE Antennas & Propagation Magazine, October 2002, Vol. 44, No. 5, October 2002, pp. 30-43.
9. S. Tourette, G. Collin, P. Le Thuc, C. Luxey, and R. Staraj, "Small Meandered PIFA Associated with SAW Passive Sensor for Monitoring Inner Temperature of a Car Exhaust Header," 2009 IEEE Transaction on Antennas & Propagation, Vol. 57, No. 9, September 2009.
10. Rashid Ahmad Bhatti, Yun-Taek Im, and Seong-Ook Park, "Compact PIFA for Mobile Terminals Supporting Multiple Cellular and Non-Cellular Standards," IEEE Transaction on Antennas and Propagation, Vol. 57, No. 9, September 2009.
11. K.R. Boyle and P.G. Steeneken, "A Five-Band Reconfigurable PIFA for Mobile Phones," IEEE Transactions on Antennas & Propagation, Vol. 55, No. 11, November 2007.
12. D.M. Nashaat, H.A. Elsadek, and H. Ghali, "Single feed compact quad-band PIFA antenna for Wireless Communication Applications," IEEE Transactions on Antennas & Propagation, Vol. 53, No. 8, August 2005, pp. 2,631-2,635.
13. N.A. Saidatul, A.A.H. Azremi, R.B. Ahmad, P.J. Soh, and F. Malek "A Development of Fractal PIFA (Planar Inverted F Antenna) with Bandwidth Enhancement for Mobile Phone Applications," 2009 Loughborough Antennas and Propagation Conference.

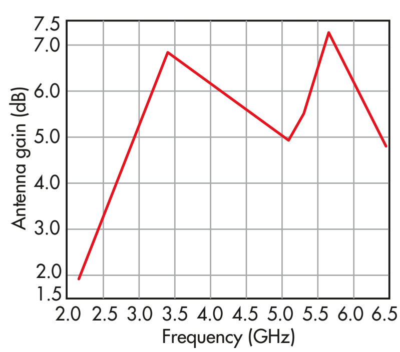

12. The simulated gain of the PIFA antenna is plotted here as a function of frequency.

Power Dividers · Couplers · Quad Hybrids · Beamformers · High Power · Milliwatts - Kilowatts

At TRM Microwave, we partner with your team to engineer innovative, custom designs for every project's unique needs.

Since 1970, Military, Space and Commercial Industries have relied on TRM's ingenuity for numerous program applications.

We are committed to continuous service over the lifecycle of every part, project, and idea we complete.

Let's Start Something.

TRM MICROWAVE
COMPLETING YOUR IDEAS®

SBA WOSB
Woman Owned Small Business

Proud to be a Woman-Owned Small Business
Custom Passive RF Components Since 1970.
ISO 9001:2008 Certified

www.trmmicrowave.com Apps Engineering Support Line 888.677.6877 info@TRMMicrowave.com

JACK BROWNE | Technical Contributor

Selecting Electromechanical and Solid-State RF SWITCHES

Due to differences in key characteristics between electromechanical and solid-state RF/microwave switches, designers must choose wisely to meet application demands.

Switches provide control in RF/microwave systems, turning power on and off and channeling signals from one branch of a circuit or system to another. They come in many shapes and sizes, and are based on a number of technologies, changing contacts by electromechanical functions or by the electronic behavior of semiconductors like PIN diodes and field-effect transistors (FETs).

Generally, solid-state semiconductor-based switches are smaller and lighter than mechanical models, and can fit into tighter spaces in a circuit layout. Solid-state switches are also capable of fast switching speeds compared to mechanical switches. But the small size usually means a compromise in power-handling capability compared to a larger electromechanical switch.

1. Waveguide switches can be implemented with either electromechanical or solid-state switching functions. (*Courtesy of Logus Microwave*)

Also, the continued maturity of microelectromechanical-systems (MEMS) switches in recent years has provided a switch technology that falls midway between the characteristics of solid-state and conventional electromechanical switches. They feature mechanical switching operation with the small feature sizes associated with semiconductors.

GOING ELECTROMECHANICAL

Why choose one RF/microwave switch type over another? In some applications, where there is a clear need to channel high-power signals, such as continuous-wave (CW) power levels of hundreds of watts or peak power levels of thousands of watts or more, the limited (millisecond) switching speed of an electromechanical switch may prove adequate for many systems. Such switches are capable of extremely broad continuous frequency ranges, such as the dc-to-18-GHz range common to electronic-warfare (EW) and military-radar applications.

Electromechanical switches incorporate some form of physically moving switch contact to close a circuit and transfer signals from one part of a switch component to another. For higher-power applications, these switches are typically constructed with waveguide interconnections *(Fig. 1)* for use in specific waveguide frequency bands, often for satellite-communications (satcom) systems.

Of course, all electromechanical switches are not created equal. Depending on the configuration, they may not be suitable for hot-switching of high-power signals. A rotary electromechanical switch, for example, rotates an electrical contact among different switch positions. When it is between positions, however, it presents an infinite voltage standing wave ratio (VSWR) to the source, with the switch essentially acting as a termination for high-power signals and ultimately suffering damage. For that reason, the hot-switching power rating of any type of RF/microwave switch should be confirmed before it is specified for any application requiring high-power hot switching.

SOLID-STATE TAKES ON KILOWATT POWER

For high-power pulsed applications, such as in radar systems, solid-state switches based on PIN-diode switch elements have shown the ability to handle kilowatts of peak power through microwave frequencies. In such a switch, a PIN diode allows current to flow with low impedance in one direction (when biased with a posi-

2. Coaxial switches can incorporate a simple toggle switch for control. ***(Courtesy of Logus Microwave)***

tive voltage) while blocking the flow of current with a high impedance in the other direction (when biased with a negative control voltage).

Although PIN-diode switches may lack the high average power-handling capabilities of electromechanical switches, they are capable of somewhat faster switching speed in the microsecond range. PIN-diode switches typically achieve high off-state isolation of better than 40 dB with low insertion loss in the on state.

This tradeoff of switching speed for power-handling capability continues with solid-state switches based on GaAs FET nonlinear switching elements, which can reach nanosecond switching speeds, but typically less than 1 W (+30 dBm) signal power. GaAs switches are capable of extremely broadband operation through 40 GHz, depending on the interconnection. They also offer lower-frequency (down to dc) operation than PIN-diode switches, when dc-coupled operation is required. On top of that, GaAs switches tend to suffer less from video leakage between switch ports than PIN-diode switches.

In terms of package styles, both solid-state and electromechanical switches come in housings with coaxial or waveguide interconnections *(Fig. 2)*. However, they are also being designed more frequently into drop-in or surface-mount-technology (SMT) packages to support design miniaturization *(Fig. 3)*. All types of switches may include internal terminations or rely on external terminations to properly terminate an unused switch port in a system's characteristic impedance, typically 50 Ω for RF/microwave systems and 75 Ω for cable-television (CATV) systems.

The switches generally have different numbers of poles and throws, such as single-pole, single-throw (SPST) and single-pole, double-throw (SPDT), and as absorptive or reflective units and with latching or failsafe switching. Absorptive switches present a low VSWR at the unselected switch port; reflective switches have a high VSWR at any unselected signal path. A failsafe switch features a default position and requires applied power to change to another switch position. With loss of power, it returns to the default position, whether normally open or closed.

A latching switch, on the other hand, will draw current to maintain a position, using a pulsed dc voltage command to change positions. When a latching switch loses power, it will remain in its last position. This switch requires power to change positions, but does not require power to remain in each position.

SWITCHES WITH MAGNETIC PERSONALITIES

Electromechanical switches have evolved to achieve higher operating lifetimes using magnetic rather than purely mechanical contact motions. Magnetic switching results in less mechanical wear, extending what was once considered a normal switch lifetime of 100,000 switching operations to much longer lifetimes of typically millions of switching operations. Less physical wear also means less performance degradation over time, with consistent performance provided for essential switch performance parameters such as insertion loss, isolation, and VSWR, even after millions of switching operations.

3. An increasing number of solid-state and electromechanical switches are housed in SMT housings to facilitate circuit miniaturization. *(Courtesy of Skyworks Solutions)*

Another type of electromechanical switch that employs the use of magnetic actuation is the ferrite switch, which is actually a form of electrically reversible ferrite circulator. It uses magnetic fields to change switch positions, with applied current magnetizing a resonator formed of ferrite substrate material. In terms of power-handling capability, a ferrite switch is typically somewhere between a rotary electromechanical switch and a PIN diode switch, and has been used in applications such as fire-control radar systems that use multiple antennas for identification. A ferrite switch enables the use of a single signal source for multiple radar system antennas.

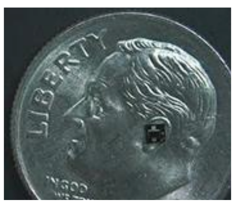

4. RF switches based on MEMS technology combine many of the features of electromechanical and solid-state switches. *(Courtesy of Radant MEMS)*

Ferrite materials have also been the basis for toroidal waveguide switches, where multiple phase shifters are used to achieve the switching function. By incorporating a waveguide tee, input signals can be divided, shifted in phase, and then recombined for addition or subtraction, depending on the output port. The choice of ferrite materials in such switch designs is critical, since operating power and temperature can affect performance, with increased insertion loss often occurring at elevated power levels.

A MEMS APPROACH

High-frequency switching functions have also been implemented with MEMS technology, which combines many of the benefits of solid-state and electromechanical approaches. MEMS switches are electromechanical in nature, with low loss, high isolation, and long operating lifetimes, but are fabricated with semiconductor-type processes and dimensions *(Fig. 4)*.

MEMS switches, which consist of electronic and mechanical sections, offer the reliability of millions of switching operations and frequency operation into the millimeter-wave region. Switch actuation is most often by electrostatic means, although MEMS switches have also been designed with magnetostatic and piezoelectric switch actuation. They are capable of microsecond switching speeds with reasonable isolation and relatively low loss. MEMS switches have gained favor in portable and mobile electronic designs due to their small size, low power consumption, and relatively low cost. mw

UNCOVER MASSIVE MIMO TECHNOLOGY CHALLENGES

FIFTH-GENERATION (5G) NETWORKS are expected to utilize advanced technology to fulfill lofty expectations. Specifically, massive multiple input, multiple output (MIMO) antenna schemes are likely to be implemented to satisfy future demands. The application note, "Examining the Challenges in Implementing and Testing Massive MIMO for 5G" from Keysight Technologies, begins with a review of the MIMO process. It then discusses some of the challenges associated with implementing massive MIMO, as well as challenges and solutions involved in the simulation, design, and testing of massive MIMO systems.

Keysight Technologies, 1400 Fountaingrove Pkwy., Santa Rosa, CA 95403; (707) 577-2663; www.keysight.com

The application note begins by describing four types of antenna systems: single input; single output (SISO); single input, multiple output (SIMO); multiple input, single output (MISO); and multiple input, multiple output (MIMO). After describing single-user MIMO in some detail, multi-user MIMO is then explained. Some differences between single-user and multi-user MIMO are discussed. An illustration is included to demonstrate how using more antenna elements, as well as applying a phase shift, can impact a transmitted signal.

An overview is provided of the massive MIMO process in a time-division-duplex (TDD) system. Next, two massive MIMO MATLAB simulations are presented, each with four users and one base station. In both examples, each user-equipment (UE) has a single antenna, while the base station contains a multi-antenna array. The base station in the first simulation example has a linear array of 50 omni-directional antenna elements, while the second example's base station has a linear array of 200 omni-directional antenna elements. The results from both simulations are presented.

Three challenges are discussed in terms of implementing massive MIMO: reciprocity error, signal-to-interference ratio (SIR), and channel coherence time. Challenges and solutions associated with massive MIMO testing are then discussed. For example, test equipment must accommodate the needs for higher frequencies and wider bandwidths. Test methods also must support the tens to hundreds of antennas that are likely to accompany massive MIMO designs. Lastly, the document describes Keysight's real-time beamforming measurement system, which consists of both hardware and software solutions.

TECHNOLOGY TRANSFORMS HOMES INTO SMART HOMES

A REPORT COMPILED from nearly 1,300 U.S. consumers in April 2016 provided insight in terms of why customers are interested in smart-home services, what features they really want, and how they intend to use smart-home technologies. According to the report, the real desire of consumers is services, or smart home as a service (SHaaS), as opposed to a collection of connected devices. SHaaS is the subject of Qorvo's white paper titled, "What is SHaaS? And why should you care?"

Home automation devices have actually existed for decades, allowing people to remotely control doors, windows, environment, entertainment, etc. The X10 communication protocol, which was introduced in the 1970s, enabled wireless control of a wide range of in-home devices. The document asserts that many of today's smart-home devices are only slightly more sophisticated than X10 systems, with a smartphone being used in place of—or in addition to—a local remote control.

Converting a basic connected device to a smart device requires three additional capabilities. First, the device must connect to and communicate with other smart/connected devices in the home. It also needs to be intelligent, meaning that a smart-home solution must recognize a home's normal behavior so that proper action can be taken when something unexpected occurs. Lastly, all functions need to be managed from a single application on a web-connected device, such as a smartphone or tablet.

Utilizing a SHaaS ecosystem can reduce redundancy and maintenance. For example, a single sensor can be used for a range of applications. A motion sensor could be used to control lighting, manage the home environment, and more.

Qorvo Inc., 2300 NE Brookwood Parkway, Hillsboro, OR 97124; (844) 890-8163; www.qorvo.com

A description of four basic components in a SHaaS application is provided. The first component is a network of sensors in the home. Secondly, a local hub wirelessly collects the information derived from these sensors. This information is securely transmitted to an intelligent cloud service that collects and analyzes the data. A central management app for the consumer and service-provider support are the third and fourth components, respectively.

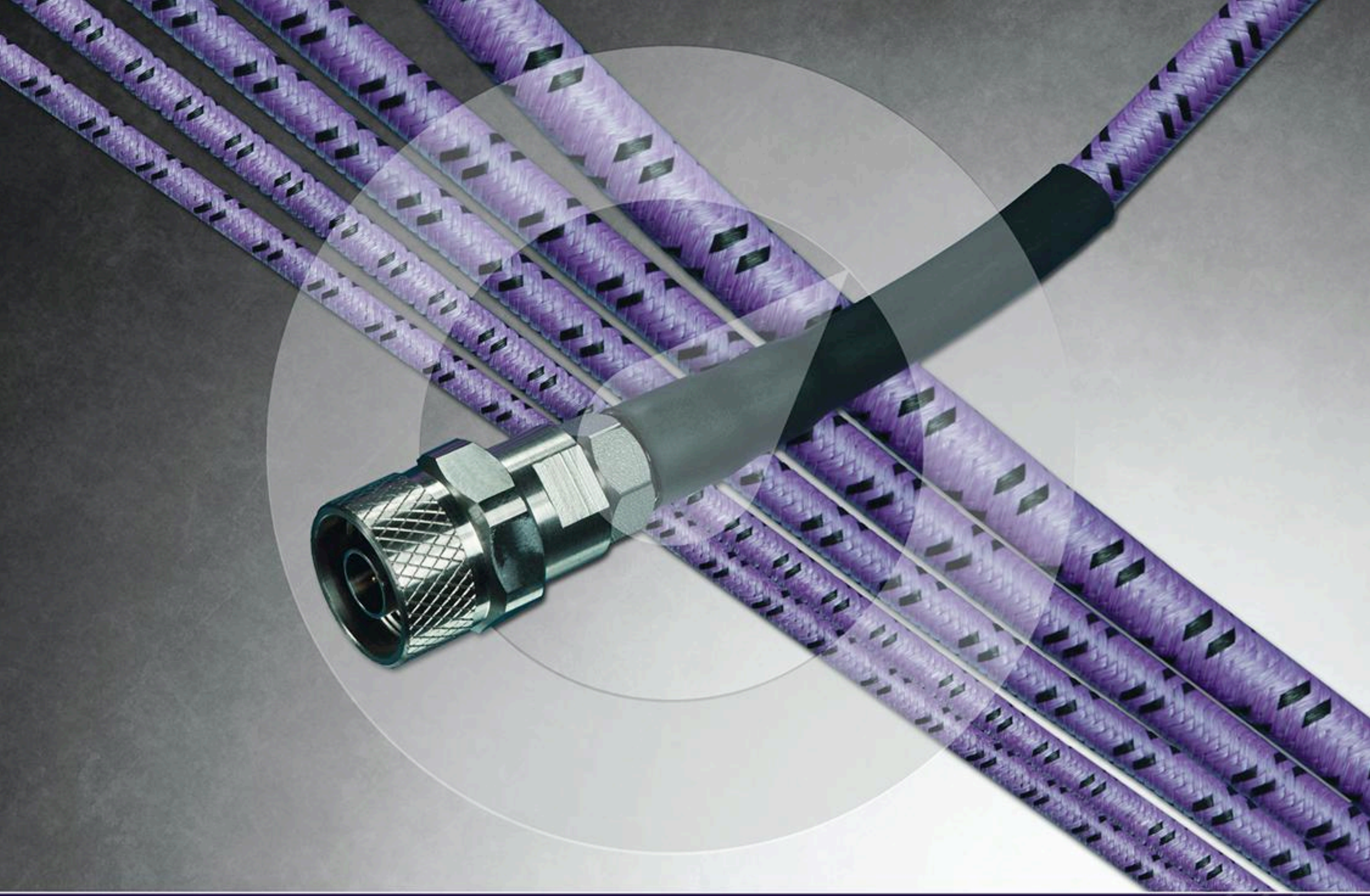

Performance Over Time

You can't afford to wonder if your cables are impacting your results. You expect your cables to be reliable. You need your cables to last.

But, with 75% of cables failing during installation or operation, your cable selection needs to be more than an afterthought. Choosing authentic GORE® Microwave/RF Test Assemblies is the only way to be sure your cables will stand up to the rigors of everyday use in demanding applications.

GORE® PHASEFLEX® Microwave/RF Test Assemblies – for proven performance, time and again. Learn what sets GORE® Microwave/RF Test Assemblies apart at:

www.gore.com/test

Insist on authentic GORE® Microwave/RF Test Assemblies – the proven purple performer.

GORE
Creative Technologies Worldwide

precision repeatability durability

Follow us on

Cover Story

JACK BROWNE | Contributing Editor

RF Measurement Modularity REDEFINED

The second generation of a vector signal transceiver (VST) module reduces the physical size of the first-generation instrument while increasing its performance and functionality.

1. The PXIe-5840R vector signal transceiver packs what once required a rack of instruments into a two-slot PXIe instrument module capable of 1-GHz instantaneous analysis bandwidth from 9 kHz to 6.5 GHz.

MODULAR TEST SYSTEMS can require some imagination, especially in terms of how much measurement functionality is possible in such little space. With PXIe instrument modules, for example, a test system with signal generators and analyzers occupies a fraction of the volume of traditional "one-box" instruments. What used to occupy a full 19-in. rack can now fit right beside a computer on a workbench. The first-generation model PXIe-5644R vector signal transceiver (VST) from National Instruments was impressive, fitting a test system within three PXIe slots. The firm's second-generation model PXIe-5840 VST is even more amazing, extending frequency, bandwidth, and overall performance of the first-generation VST in 33% less volume (just two PXIe slots) while adding a fifth virtual instrument, a high-speed serial bus. What was once a large rack of instruments is now a handful of measurement power.

As with the first-generation PXIe-5644R VST, the PXIe-5840 VST (*Fig. 1*) requires a new way of thinking about test equipment and electronic systems. In terms of functionality and performance, the new VST is loaded, with a 1-GHz instantaneous analysis bandwidth that can be tuned from 9 kHz to 6.5 GHz. It is a complete hardware system that fits within a pair of PXIe chassis slots—and a large part of that volume is devoted to heat sinking and thermal management. The PXIe-5840 VST includes a fast-switching signal generator/transmitter and wideband receiver or analyzer as well as a user-programmable field-programmable gate array (FPGA) and a high-speed digital interface that allows the rapid transfer of data for diverse applications, from signal and channel monitoring to research and/or production test-and-measurement use.

In many ways, the PXIe-5840R VST is the logical conclusion of combining a PC with a system-level approach to test and measurement. The PXIe module contains the usual input and output test ports found on a one-box instrument, including for reference oscillators and local oscillator (LO) signals as needed for frequency upconversion and downconversion of signals of interest. But there are none of the bells and whistles that usually crowd the front panel of a conventional one-box analyzer. Instead, control and adjustments take place on a PC or other computing device and results are shown on a PC screen. The PC or other computing device orchestrates the measurement functions by running suitable measurement/monitoring software, such as the popular LabVIEW system-design software from National Instruments.

By drawing upon the flexible LabVIEW software for measurement definition, the test capabilities of the PXIe-5840R VST can be redefined in the time it takes to change settings in software or download an example application from a library of programs compiled by the growing LabVIEW user base. The beauty of the PXIe modular instrument format is its ease in expanding a test system's inputs and outputs, by adding modules to a chassis. This can be particularly useful for applications such as testing antenna arrays or multiple-input, multiple-output (MIMO) antenna systems. When a device under test (DUT) is for an existing communications standard, such as Bluetooth or Wi-Fi, more than likely the required set of measurements for compliance to that standard can be found ready for download in the LabVIEW software library.

SAVING TIME AND SPACE

In addition to the compact footprint provided by PXIe systems, there is also an associated savings of time in setting up a system for a particular measurement. For multiple-channel, phase-sensitive measurements, for example, which would normally require great attention to a choice of properly phase-matched coaxial cables maintained within a controlled-temperature environment, the interconnections in a PXIe system take place on the measurement chassis backplane, with the tight tolerances for amplitude, phase, and timing synchronization among multiple test channels already defined by the PXIe backplane specifications.

Admittedly, some engineers may prefer the simplicity of a single box, such as a digital storage oscilloscope (DSO) and a trusted set of probes, over the almost unbounded measurement capability afforded by a software-driven, modular system built around the PXIe-5840R VST. For troubleshooting or simple measurements, a one-function box offers the simplicity of a limited set of measurement options. But as modern electronic components grow in complexity and continue to integrate functionality within smaller package sizes, measurements also grow in complexity. Having a large part of an automatic-test-equipment (ATE) system block diagram within two slots of a PXIe chassis, such as with the PXIe-5840R VST, erases questions about finding the right test signal source or if the test signal level is sufficient for properly evaluating passive components, such as filters.

The PXIe-5840R VST embodies numerous performance improvements over the company's first-generation VSTs, not to mention the reduction in physical size. The frequency range of 9 kHz to 6.5 GHz covers many commercial wireless communications bands, including Third-Generation (3G) and Fourth-Generation (4G) cellular radio frequencies. Access to the VST's internal LO allows the use of a frequency-extension module mounted alongside the VST in a PXIe chassis to extend the usable frequency range into the millimeter-wave range for such applications as commercial automotive radar testing. The 1-GHz instantaneous bandwidth of the VST's receiver is a tremendous aid for testing applications with wideband modulation or for evaluating different measures used in RF/microwave amplifiers to enhance linearity, such as digital predistortion (DPD), that can quickly consume bandwidth.

The PXIe-5840R delivers a healthy amount of vector signal generator (VSG) power, typically +23 dBm continuous-wave (CW) power at 1 GHz or about 10 dB more power than the first-generation VSTs. The PXIe-5840R's vector signal analyzer (VSA) boasts ±0.35 dB amplitude accuracy in its measurements for highly accurate gain and loss measurements. With the growing complexity of RF-related measurements for wireless mobile devices, the PXIe-5840R can deliver data in a hurry, with better than 200 µs frequency tuning speed or a better than 33% improvement in tuning speed over the first generation.

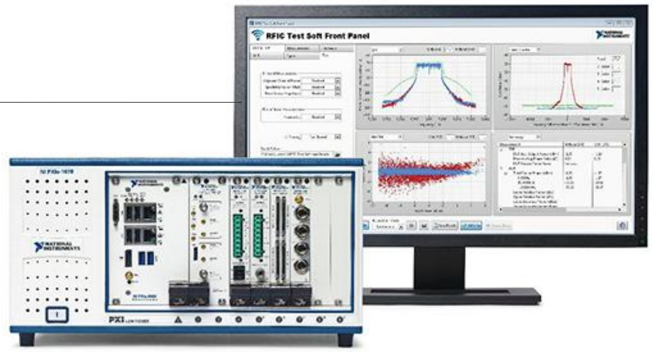

2. The "soft front panel" provided by the LabVIEW GUI helps to speed and simplify advanced component testing with the PXIe-5840R VST and other PXIe instrument modules.

Availability of an instrument module like the PXIe-5840R tends to blur any distinction between what is a test instrument and what was once known as an ATE system. The VST is essentially both, a software-defined measurement tool that can be programmed by a user. It is powered internally by a Virtex 7 X690T FPGA from Xilinx (www.xilinx.com) to accept user instructions on how to perform a measurement. The fast tuning speed and lack of latency within the PXIe-5840R make it possible to collect comprehensive test results across wide measurement bandwidths, with more data points for analysis in shorter measurement times.

What was once an ATE system typically involved one or more racks of single-function test instruments and custom software that would be used to perform specialized automated measurements, such as amplifier gain and output power as functions of frequency. The large racks are no longer needed and the custom software has been replaced by the user's instructions, whether from LabVIEW or some other program. For users of LabVIEW, the firm offers a number of different test examples and case studies that serve as starting points for users seeking rapid development of a test solution using LabVIEW with the PXIe function modules. For example, the modules and software have been used by organizations such as NASA to shave hours off the development time of creating specialized automated measurements on microelectromechanical-systems' (MEMS) space-based components.

The NI PXIe-5840 VST not only performs measurements quickly, it can move the test results quickly via an eight-channel parallel 50-MHz wide parallel digital port as well as a four-channel bidirectional high-speed serial interface capable of 12 Gb/s data transfer speed. It can be teamed with other PXI modules, such as source-measure units and VSAs, for advanced measurement capabilities within a single PXIe chassis. The LabVIEW GUI serves as what the company calls a "soft front panel" to help guide users in setting up even advanced measurements on amplifiers with DPD and envelope tracking (*Fig. 2*). Whether for research or production, the next-generation NI PXIe-5840R VST represents a next step in the way to perform high-frequency measurements quickly and effectively. mw

---

NATIONAL INSTRUMENTS, 11500 N. Mopac Expressway, Austin, TX 78759-3504; (512) 683-0100, www.ni.com.

JOHANA YAN | Lead Engineer
MaXentric Technologies, www.maxentric.com

Optimizing Design of Envelope-Tracking Power Amplifiers for 4G/5G

By utilizing the proper hardware and software, the envelope-tracking technique can be implemented to enhance power amplifier performance.

THE NEED FOR greater spectral efficiency among next-generation communication standards, such as 4G/5G, has led to the use of more complex modulation schemes to address an increasing demand for higher data rates. Older modulation schemes based on phase or frequency modulation with no amplitude information carried on the signal could be supported by power amplifiers (PAs) driven into compression, and thus operating at higher levels of power-added efficiency (PAE).

BLOCK DIAGRAM OF THE NI PXI ENVELOPE-TRACKING POWER AMPLIFIER TESTBENCH

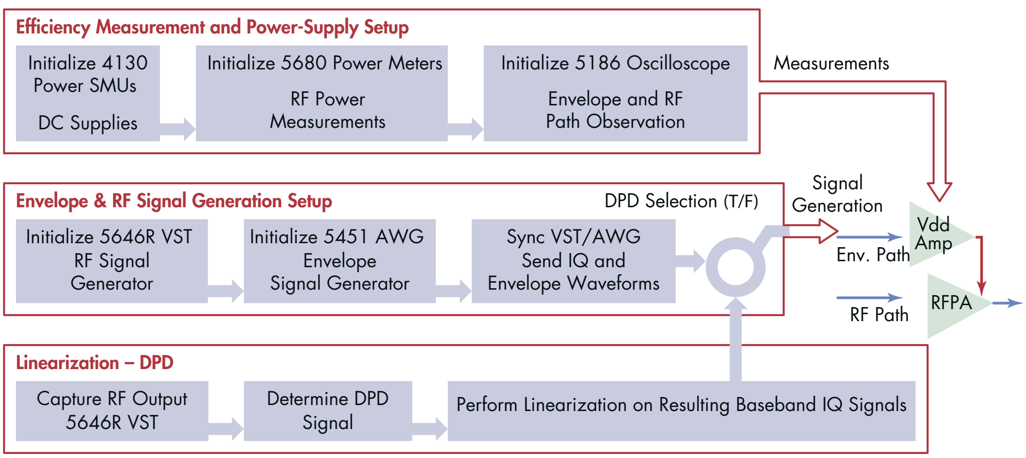

1. This is a diagram of the NI PXI ETPA testbench.

However, due to the need for spectral efficiency, modulation schemes that include amplitude variations lead to signals with non-constant envelope and high peak-to-average signal ratio, resulting in PAs that frequently operate below their compression point and at lower PAE values.

The efficiency of the PA determines the power consumption, size, and battery lifetime of the radio. Various techniques, such as envelope tracking (ET), have been explored to increase the efficiency of PAs for high peak-to-average power ratio (PAPR). ET adjusts the supply voltage applied to an RF PA to deliver the power needed at that instant.

This article describes the development of an envelope-tracking power amplifier (ETPA) testbench capability for real-time efficiency and linearity measurements for optimizing ETPA design, along with flexibility to accommodate different 5G signals. This capability uses NI LabVIEW software to test and optimize the ETPA, in addition to a vector signal transceiver (VST) for RF signal generation and an arbitrary waveform generator (AWG) for envelope signal generation. The design, on-board retuning, and final optimization are performed with the NI AWR Design Environment.

ET technology enables operators to utilize only as much power as is necessary to provide the amplified output. This technology reduces energy consumption, thus significantly lowering operating costs while providing environmental sustainability. In addition, from the hardware system perspective, this allows a smaller form factor and higher reliability due to lower junction temperatures, as well as much lower weight due to reduced battery and energy requirements.

Aside from designing for high efficiency, today's PA designers must be concerned about amplifier linearity maintaining signal integrity in a crowded frequency-spectrum allocation. High linearity is required in these communication systems in order to minimize signal distortion and reduce bit error rate

2. This integrated envelope modulator is designed for micro base stations.

(BER), as well as reduce adjacent channel interference.

ADVANTAGES OF NI PXI HARDWARE AND LABVIEW SOFTWARE

Traditional testbenches are made to test PAs with a constant supply voltage. With ET, a modulator is used as a dynamic power supply that varies as a function of the signal's envelope. This technique is deliberately designed for signals with high PAPR; hence, traditional PA tests cannot be used to validate their performance. Communication systems need to be developed based on the average performance of an ETPA operating under typical modulation conditions, as opposed to continuous-wave (CW) performance at the peak supply voltage. The problem is further complicated by the lack of accurate simulation models over a wide range of supply voltages. Most device models are valid at the nominal constant supply voltage ±10%. With ET, the supply voltage can be 90% lower than the peak supply voltage. Thus, real-time performance measurements are highly desired for optimizing the ETPA.

Testbenches built in the past have taken a year or more to complete. With NI's integration and the use of LabVIEW, the designers were able to complete the NI ET testbench in less than two months. An important feature offered by PXI is the ease of synchronization between equipment modules.

Due to the nature of ET, it is critical that the supply envelope signal arrive at a specific time with respect to the RF signal. Additionally, 5G PAs need to support various types of modulations, which the VST can generate. Another advantage of the VST is its wide frequency range of 65 MHz to 6 GHz. And with 200 MHz of instantaneous bandwidth, the VST allows system flexibility for various applications.

Because envelope tracking is inherently wideband in terms of tunable RF bandwidth, a wideband ETPA with this NI ET testbench can be used to test various LTE bands, GPS, and military applications—all in the same day, with simply a click to change the RF frequency.

OPTIMIZING WITH THE VST AND MICROWAVE OFFICE SOFTWARE

To develop a testbench for optimizing envelope tracking, the various modules shown in *Fig. 1* were used. Power source measurement units (SMUs) were employed to allow for real-time dc-power-consumption measurements. The RF power meters enabled engineers to monitor the input and output power. In LabVIEW, these measurements are put together and calculations are performed to allow for instantaneous monitoring of the efficiency, gain, and output power.

The envelope signal was generated using the AWG. The VST served as the RF signal generator as well as the RF feedback analyzer. The envelope-shaping relationship between the true envelope of the signal and the supply voltage was optimized easily by simply loading a different equation. In addition to addressing the PA efficiency through real-time ET, digital predistortion (DPD), using the feedback signal and MathScript, was used to improve the linearity of the ETPA.

To further improve the performance, impedance tuning was applied based on information derived from load and source pulling with external tuners. The Microwave Office software was used to apply the optimized tuning to the onboard ETPA RF matching circuitry. The

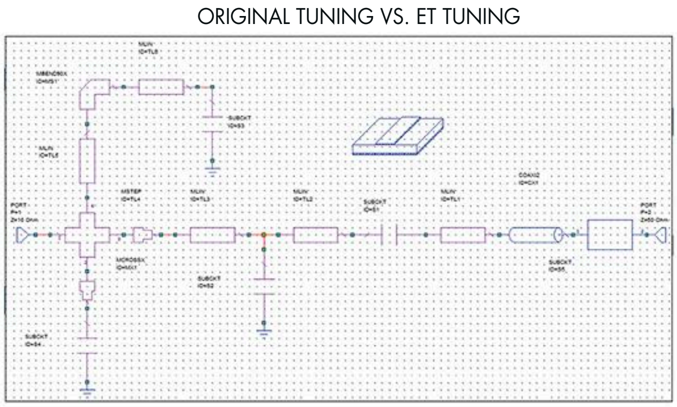

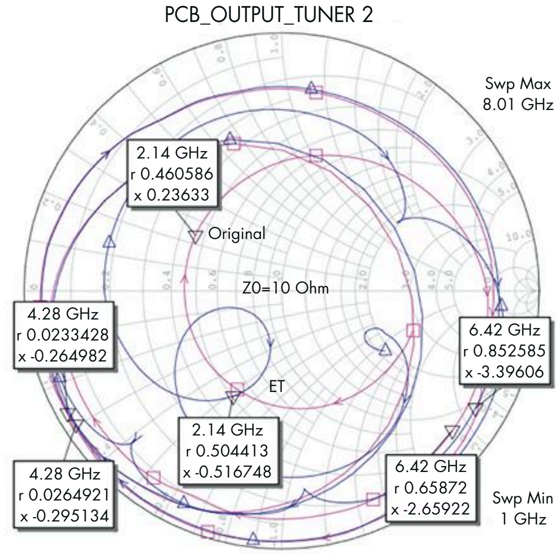

3. The ETPA was retuned using the Microwave Office software.

reduced characterization time and capability to optimize the ETPA in real-time is a significant game-changer for power-amplifier designers.

The time alignment of the amplitude signal and RF signal at the RF transistor is critical for optimizing the ETPA's performance. A time misalignment in these two signals will produce signal distortion, degrade adjacent channel power ratio (ACPR) performance, and reduce efficiency. Characterization of the time-delay difference between these two signal paths will allow for time alignment.

This delay difference may vary with temperature or aging. Therefore, the system needs to compensate for this variation to ensure optimum performance. Using NI's PXI, VST, AWG, and LabVIEW, the designers were able to visually see the improvement/degradation in linearity and efficiency as the alignment between the RF signal and the envelope supply was altered in real-time.

RESULTS OF ENVELOPE TRACKING

The NI VST and PXI were used to optimize the LTE Band 1 (2.14 GHz) PA using MaXentric's MaXEA 1.0 modulator *(Fig. 2)*. The MaXEA 1.0, designed for micro base stations, is a 30-V integrated envelope modulator with greater than 70% modulator efficiency. It can deliver up to 7 W of average envelope output power. It is designed to support signals with high PAPRs, such as those used in 4G/5G. The MaXEA 1.0 is compatible with various PA technologies—among them, laterally diffused metal-oxide semiconductor (LDMOS), gallium nitride (GaN), and gallium arsenide (GaAs).

In this example, a GaN device was employed for the PA design. The PA was tuned and optimized for ET operation using the NI PXI system. Initial output and input external tuners were used to optimize the efficiency, gain, and output power of the ETPA. The desired input and output impedances were measured with a vector network analyzer (VNA).

Microstrip-based board matching circuits were designed and simulated with Microwave Office *(Fig. 3)*. The retuned ETPA was then measured again using the PXI, VST, and LabVIEW ET setup to confirm its performance. Time alignment between the RF (VST) and the envelope (AWG) paths was performed digitally in LabVIEW for best efficiency and linearity.

Without linearization, the ETPA achieved 6 W of output power with 11.5 dB of gain and 53% PAE. After applying MaXentric's linearization, the output power and gain remained the same. The PAE slightly improved to 54.6%, with better than –45 dBc ACPR. To demonstrate how ET can improve efficiency and linearity, measurements were performed for the same GaN device under constant drain biasing. Achieving the same linearity performance without ET required the input power to be significantly reduced. The results were a low efficiency of 6.1% at 0.5-W output power without DPD and 22.5% efficiency at 2 W of output power with DPD. *Figure 4* shows the MaXentric ETPA with MaXEA (a), the spectra before and after MaXPAL linearization (b), the AM/AM and AM/PM before MaXPAL linearization (c), and the AM/AM and AM/PM after MaXPAL linearization (d).

CONCLUSION

Synergy between NI's measurement equipment and NI AWR Design Environment enabled the ETPA's design success. This solution helped the designers significantly reduce PA optimization time without sacrificing measurement accuracy. The VST's flexibility and widely tunable RF frequency allowed the designers to design, optimize, and demonstrate wideband ETPAs across different bands and applications all in the same day. mw

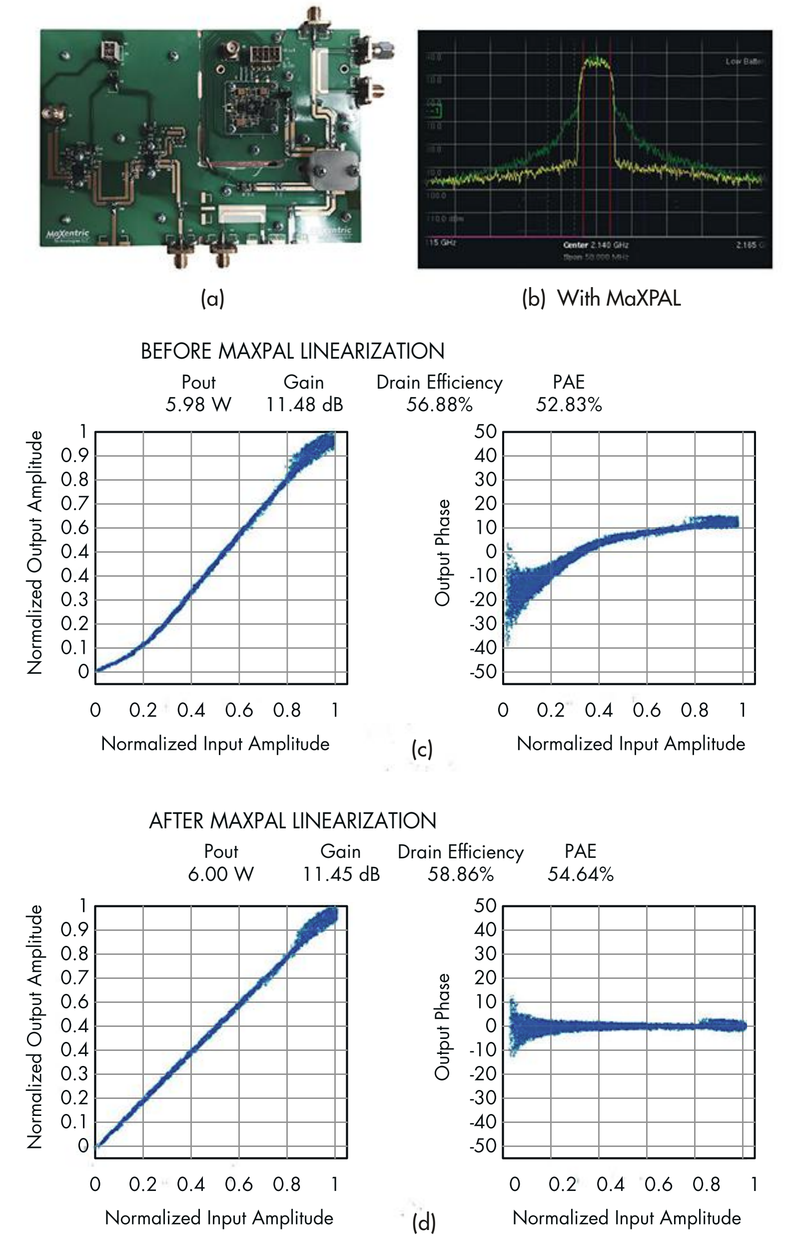

4. Shown are the ETPA with the envelope modulator (a), the spectrum both with and without MaXPAL linearization (b), AM/AM and AM/PM before MaXPAL linearization (c), and AM/AM and AM/PM after MaXPAL linearization (d).

BRAD FRIEDEN | Applications Engineer for Aerospace Defense Industry Solutions
Keysight Technologies

Improve Scope SNR Via Processing Gain

Digital downconversion and vector-signal-analysis software make it possible for an oscilloscope to view low-level pulses in the presence of much larger pulses.

PULSED SIGNAL MEASUREMENTS with an oscilloscope can become challenging when there is a lack of sufficient dynamic range and signal-to-noise ratio (SNR). In many applications, whether commercial or military, low-level pulses are often difficult to detect and measure in the presence of much larger pulses. However, using a technique to "span down" the initial 3-dB bandwidth of an oscilloscope by means of digital downconversion can greatly enhance an oscilloscope's SNR. In fact, it's possible to view two pulses separated by 50 dB in amplitude on an oscilloscope with the proper enhancements.

The help comes in the form of vector-signal-analysis (VSA) software, which processes captured data from an oscilloscope and performs digital downconversion to show low-level pulses on a log-magnitude scale—even in the presence of much larger signals. The approach helps accelerate system-validation measurements on pulsed RF signals in aerospace and defense systems, as well as in commercial and industrial radar systems. The process can markedly improve measurement accuracy when evaluating the spectral, pulse-envelope, frequency-chirp, and phase-shift characteristics of an RF pulse train.

Teaming VSA software with a digital oscilloscope significantly extends the SNR of the oscilloscope. Such software has the ability to shift captured oscilloscope RF signal samples down to baseband in-phase and quadrature (I and Q) signal components, and then apply bandpass filtering and resample the signal data at a lower sample rate to greatly reduce the noise levels. The result is a higher dynamic range and lower SNR, allowing detection of low-level signals even in the presence of higher-level signals.

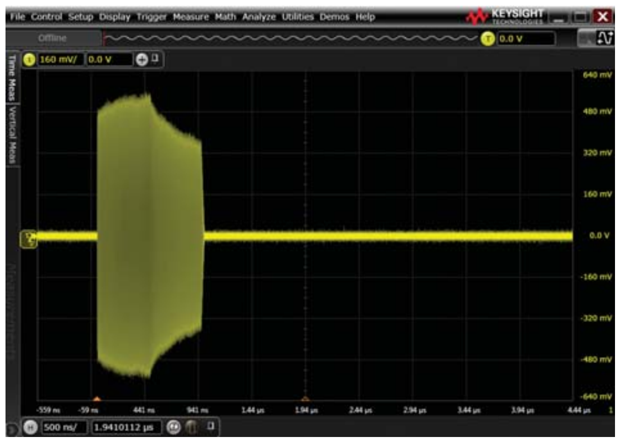

1. By using an oscilloscope with 8-GHz capture bandwidth, a +6-dBm pulse will obscure a second pulse (not visible on the display screen) that is 50 dB lower in level than the first pulse.

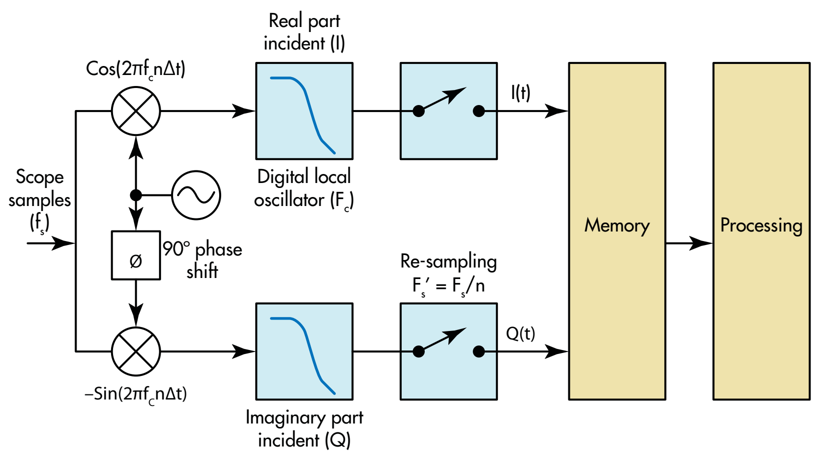

2. To improve the measurement SNR, samples captured on the oscilloscope are fed to a personal computer running the VSA software to perform digital downconversion and achieve processing gain.

SOFTWARE IN ACTION

To demonstrate the effectiveness of this approach, a wideband 8-GHz oscilloscope was employed to capture a pulse train with a large pulse, followed by a lower-level pulse that

3. **With the aid of the VSA software and center frequency, and span settings of 3.7 GHz and 500 MHz, respectively, the 50-dB down pulse is now visible.**

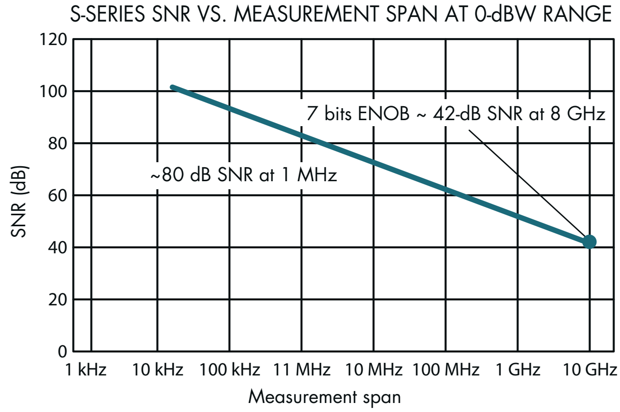

4. **This plot shows the SNR that can be achieved in a time view versus span adjustment, using the VSA software.**

is 50 dB less in amplitude. The smaller pulse is 100,000 times lower in power than the larger pulse and ≈316 times smaller in voltage $(100{,}000)^{0.5}$.

This two-pulse sequence repeats as part of the pulse train, with the lower-level pulse difficult to detect. The larger pulse has a power level of +6 dBm (about 1.4 mW), which results in a peak voltage of about 633 mV into a 50-Ω load. This is a –4-dBV peak level, or 20log(0.633). It also corresponds to a 1266-mV peak-to-peak signal into 50 Ω. In comparison, the smaller pulse—316 times smaller in voltage—is only 4 mV p-p (–44 dBm, –54 dBV peak level).

For this two-pulse example, the VSA software, which also works to control the oscilloscope front-end sensitivity, is set to +6 dBm (633 mV peak). This corresponds to a vertical measurement range of 1,266 mV on the oscilloscope. The oscilloscope has eight vertical divisions, so the setting is approximately 160 mV/div. Using the oscilloscope's full 8-GHz bandwidth at this approximate 160-mV/div setting, the broadband root-mean-square (RMS) noise is around 5 mV, interpolated from a noise chart on the oscilloscope's datasheet *(see table below)*.

That translates to 15-mV p-p noise. As a result, the smaller pulse (at only 4 mV p-p) will be masked by the instrument noise in the measurement (15 mV p-p). In turn, it will not be discerned when using the full 8-GHz measurement bandwidth of the oscilloscope, with a linear scale and no averaging *(Fig. 1)*.

DIGITAL DOWNCONVERSION

Although basic pulsed RF measurements can be made natively on a high-bandwidth oscilloscope, and there are certainly times that measurements on directly sampled signals are desired, external signal processing and analysis on captured signals can provide additional insights into measurement data. For example, a process called digital downconversion makes it possible to perform a wide range of RF pulse measurements with higher accuracy than native oscilloscope measurements, thanks primarily to the presence of lower noise due to an effect called processing gain.

Figure 2 shows the basic process of digital downconversion. By means of digital signal processing (DSP), measurement samples from the oscilloscope are multiplied by the sine and cosine of an imaginary oscillator with center frequency f_c. This DSP technique is, in effect, "tuning" to the frequency of the input signal. The process converts the time samples into real and imaginary number pairs that completely describe the behavior of the input signal.

To reduce noise, these samples can be lowpass-filtered and then resampled at a lower rate to reduce the size of the data set, allowing fast-Fourier-transform (FFT) processing of the data at a later stage. The resulting digitally downconverted samples can then be placed into memory for further processing, such as calculating the FFT.

Important demodulation data comes from this digital-downconversion process. First, when the digital local-oscillator (LO) f_c is equal to the carrier frequency of a modulated signal, then the output of the digital filters, which includes the real or in-phase signal component, I(t), and the imaginary or quadrature part, Q(t), consists of time-domain waveforms that represent the modulation on the carrier signal.

RMS LEVELS FOR 8-GHZ OSCILLOSCOPE AT DIFFERENT VERTICAL SETTINGS (V_{RMS} AC)

Vertical setting (mV/div)	S-054A (µV)	S-104A (µV)	S-204A (µV)	S-254A (µV)	S-404A (µV)	S-604A (µV)	S-804A (µV)
1	74	90	120	130	153	195	260
2	74	90	120	130	153	195	260
5	77	94	129	135	173	205	320
10	87	110	163	172	220	256	390
20	125	163	233	254	330	446	620
50	372	456	610	650	768	1300	1400
100	780	960	1200	1300	1600	2300	3100
200	1600	2000	2600	2800	3400	4900	6400
500	3500	4300	5500	6000	7300	10,000	13,300
1000	5100	6800	9200	10,100	12,500	17,600	42,100

More specifically, a mathematical representation of the captured input signal is:

$A(t)\{\cos[2\pi f_c t + \theta(t)]\}$

where the amplitude modulation, A(t), can be written as:

$A(t) \approx [I(real)^2 + Q(imaginary)^2]^{0.5}$

and the phase modulation, θ(t), can be written as:

$\theta(t) = \tan^{-1}[Q(imaginary)/I(real)]$

Displaying the I and Q results in terms of magnitude coordinates yields a view of the amplitude modulation, and showing the I and Q results in terms of phase coordinates yields a view of the phase modulation. By taking the derivative of phase modulation, frequency modulation (FM) is:

$FM = d\theta/dt$

By adjusting the width of the lowpass filters, it is possible to set a defined span around the center frequency. Here, the filter width is wide enough to pass a signal of interest, but narrow enough to filter out much of the noise that is surrounding the signal of interest.

If the oscilloscope's captured data is imported to a PC running the VSA software, it can be digitally downconverted into I and Q baseband data, bandpass-filtered, and then resampled. This process can greatly decrease the amount of noise in the measurement data. Essentially, the process "tunes" to the center frequency of the signal and then "zooms" into the signal to analyze its modulation, providing "processing gain" for the captured data.

TAKING ON TWO PULSES

For the two-pulse example, the oscilloscope's original 8-GHz-wide measurement and its associated noise are reduced to a 500-MHz-wide measurement. It is centered on the 3.7-GHz carrier with an instantaneous measurement bandwidth slightly wider than the width of the signal modulation.

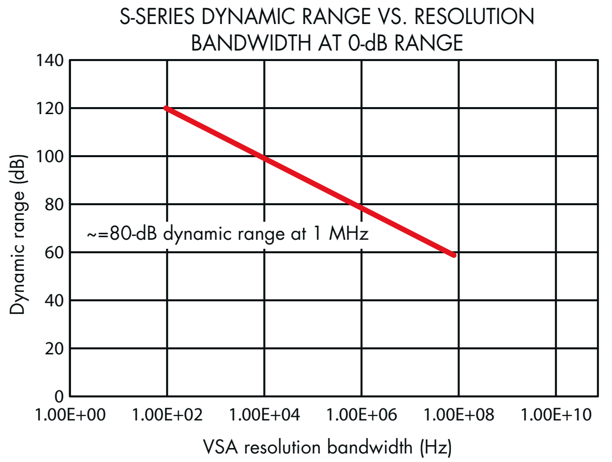

5. Dynamic range is shown in a FFT versus resolution bandwidth setting in the VSA software.

The reduction in measurement bandwidth corresponds to a SNR improvement of 10log(oscilloscope bandwidth/span) = $10\log[(8 \times 10^9)/(500 \times 10^6)] = 12$ dB. The enhanced SNR, combined with the ability of the VSA software to show a log magnitude scale and the use of averaging, makes it possible to display the smaller pulse in the presence of the larger pulse *(Fig. 3)*. *Figure 4* depicts the improvement in SNR by narrowing the span.

A similar plot can be drawn to show the improvement in dynamic range that's possible when measuring narrowband signals *(Fig. 5)*. The boost in dynamic range of 10log(oscilloscope bandwidth/span) when measuring narrowband signals in an FFT view does not fully describe the spurious-free dynamic range (SFDR) or harmonic distortion characteristics of the oscilloscope. However, it does give an idea of where the noise floor will lie in an FFT measurement. As the resolution bandwidth is decreased, the total noise is divided among smaller increments of time, resulting in the noise floor dropping. The plot of *Fig. 5* does not account for limitations due to various spurious responses; therefore, the SFDR as shown remains limited to around 50 dB. mw

JACK BROWNE | Contributing Editor

Novel Design Strategy Yields Stable SAW Filters

By applying modern filter theory to SAW filters, the process limitations of commercial SAW foundries can be included in the total design process to create low-cost, chip-scale SAW filters with BAW-like performance.

FILTERS CONTROL THE CONGESTION of modern communications signals. They are essential for preventing interference in electronic systems but can be challenging to implement, especially as mobile communications devices continue to increase functionality in ever-smaller packages. Taking a fresh look at RF filters, Resonant (www.resonant.com) applies modern design strategies such as finite-element analysis (FEA) to the creation of acoustic-resonator filters, creating surface-acoustic-wave (SAW) filters with performance comparable to bulk-acoustic-wave (BAW) filters, but in fractions of the time and cost normally required for BAW filters. Then they license rather than sell the designs to customers seeking miniature high-performance RF filters for mobile devices and other wireless products. The secret ingredient in this innovative approach to building RF filters is Resonant's Infinite Synthesized Networks (ISN) design process.

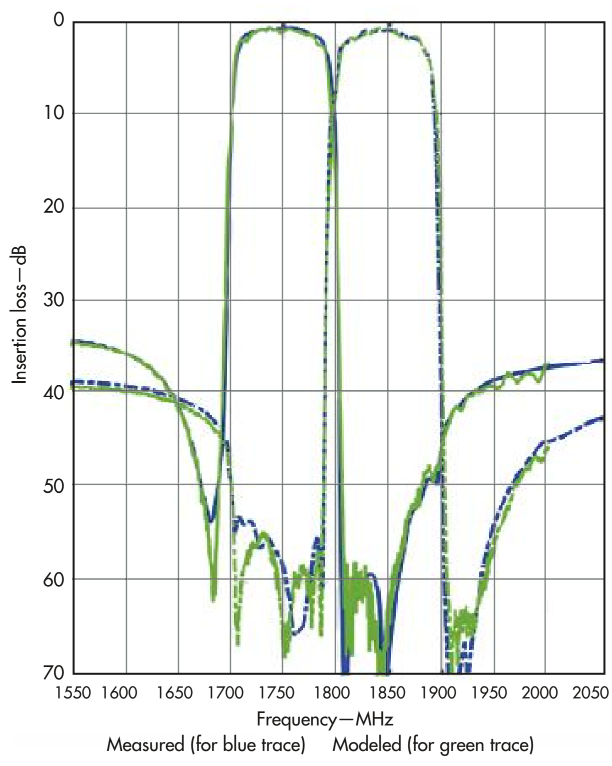

1. The two passbands of a Band 3 LTE duplexer appear closely matched between simulated and measured responses due to the accuracy of the ISN design approach.

Resonant works with commercial SAW foundries to account for known process variations as part of a filter design, to achieve BAW-like performance from commercial SAW fabrication processes. Faced with the challenge of developing a duplexer to filter the separate receive and transmit frequency bands within a 4G cellular LTE mobile handset, but not wishing to incur the cost of a BAW process, the firm relied on the ISN design approach to transcend the limitations of working with a particular SAW fabrication facility. Acoustic wave filters have traditionally employed ladder networks synthesized with the aid of foundry-based empirical models to achieve target performance levels. Under certain conditions, such as narrow operating temperatures, this can be successful. But faced with the real-world operating conditions of mobile LTE handsets, BAW filters and duplexers typically suffer less performance degradation at higher power levels and temperature extremes.

Resonant's engineers sought a means of including different behavioral mechanisms into a SAW filter design, such as linearity from high signal power levels and frequency variations due to temperature, while working within the boundaries of a given SAW device fabrication process. The ISN approach to designing SAW filters builds upon electromagnetic (EM) FEA simulation and the flexibility to modify input data to compensate for different SAW foundry lithography tolerances and variations. The ISN approach has made it possible to optimize filters for distortion-free performance with the higher-power signals typically found in LTE wireless networks and to optimize performance for different operating temperatures, including the higher temperatures produced within energy-dense LTE mobile devices.

As evidence of the effectiveness of the ISN approach, a low-cost, miniature SAW duplexer was developed for LTE Band 3 use, where the uplink (from the handset to the base station) frequency range is from 1710 to 1785 MHz and the downlink (from the base station to the handset) frequency range is from 1805 to 1880 MHz downlink. Duplexers modeled with the ISN software and then fabricated and tested at a commercial SAW foundry showed a close match between simulated and measured performance for the two passbands (*Fig. 1*).

This particular duplexer includes closely spaced passbands, where the goal is to achieve low passband loss while also providing high isolation between the passbands. Since these are miniature filters with wafer-level packaging, a commercial wafer prober and vector network analyzer (VNA) are enlisted for the measurements, gauging loss from antenna to transmit port and antenna to receive port for realistic values. The typical loss for an individual duplexer in the center of each passband was 0.9 dB, with loss rising to no more than 2.2 dB at the transmit frequency band edges (critical for power amplifier efficiency). The isolation between passbands was typically 54 dB.

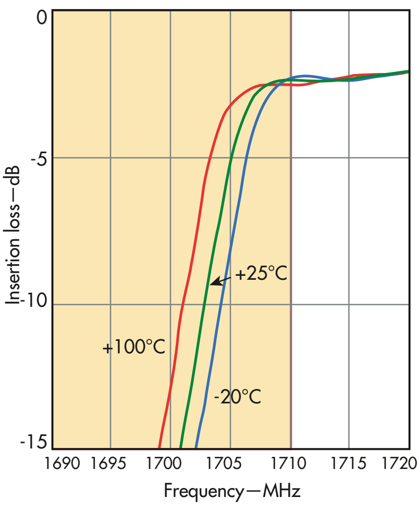

2. Even for SAW substrate materials, the effects of temperature can be minimized for SAW filters and duplexers.

Perhaps even more impressive was how little the insertion-loss performance varied with frequency as a function of temperature, when measured across a wide range from -25°C to 100°C. Designed with the Resonant ISN tools, the passband responses of these SAW duplexers changed 3.4 MHz in frequency for that wide temperature range, or a shift of only 17 ppm/°C (*Fig. 2*). The ISN design tools can model the characteristics of lithium tantalate and composite/bonded substrate materials used by commercial SAW foundries to account for the effects of temperature and power, and create designs that maintain high linearity even at higher power levels such as those found in 4G LTE handsets. The filters and duplexers are also quite compact, measuring just 1.8 × 1.4 × 0.38 mm to fit the high-density packaging requirements of modern smartphones and mobile devices. The ISN design process is available in a free, downloadable white paper available from the Resonant website. mw

RESONANT INC., 110 Castilian Dr., Ste. 100, Goleta, CA 93117; (805) 308-9803, www.resonant.com.

JACK BROWNE | Technical Contributor

High-Speed DACs Deliver Agile RF/MW Signals

Targeting wireless infrastructure applications, these converters provide up to 16-b resolution for creating wide-dynamic-range signals as high as 7.5 GHz.

DIGITAL-TO-ANALOG CONVERTERS (DACs) have been used for many years to generate lower-frequency signals. However, they typically lacked the sampling speeds and precision needed for recreating RF/microwave signals with any form of moderately complex modulation—until, that is, the arrival of the 11-b AD9161 and 16-b AD9162 DACs from Analog Devices. Both are capable of direct RF signal synthesis at speeds of 6 Gsamples/s and more, and update rates of 12 Gsamples/s for crafting signals at frequencies to 7.5 GHz.

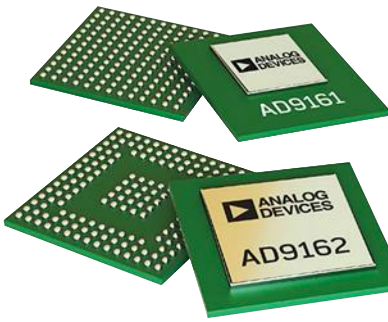

The AD9161 and AD9162 DACs run at update rates as high as 12 Gsamples/s to generate outputs reaching 7.5 GHz.

The AD9161 and AD9162 *(see figure)* can produce wideband modulated signals for use in wireless infrastructure and DOCSIS 3.1 cable applications. Both DACs are based on a quad switch architecture that employs a 2× interpolator filter for update rates to 12 Gsamples/s in some modes. The interpolator filter also allows them to be configured for power-conserving lower data rates and clock speeds that simplify the filtering requirements.

The two DACs can construct waveforms in the second and third Nyquist zones at frequencies up to 7.5 GHz while maintaining excellent dynamic range and low-noise performance.

DACs DEAL WITH DOCSIS

These two high-speed DACs are designed to produce wide-dynamic-range signals for wireless infrastructure and single- and multiple-carrier data over cable service interface specification (DOCSIS) applications. For example, operating at a DAC frequency of 5 Gsamples/s, the AD9161 achieves a spurious-free dynamic range (SFDR) of –82 dBc for an output frequency of 70 MHz, –70 dBc for an output frequency of 2 GHz, and –55 dBc for an output frequency of 4 GHz. For DOCSIS applications at the same DAC frequency, the SFDR is –70 dBc for a single carrier at 70 MHz, –68 dBc for four carriers at 70 MHz, and –65 dBc for eight carriers at 70 MHz. At 950 MHz, the SFDR is –70 dBc for a single carrier, –68 dBc for four carriers, and –64 dBc for eight carriers.

The higher-resolution AD9162 offers comparable SFDR performance in similar conditions, with SFDR of –82 dBc for an output frequency of 70 MHz, –70 dBc for an output frequency of 2 GHz, and –60 dBc for an output frequency of 4 GHz. For DOCSIS applications, the SFDR is –70 dBc for a single carrier at 70 MHz, –70 dBc for four carriers at 70 MHz, and –67 dBc for eight carriers at 70 MHz. At 950 MHz, the SFDR is –70 dBc for a single carrier, –68 dBc for four carriers, and –64 dBc for eight carriers.

The adjacent-channel-power performance of the AD9161, for an output frequency of 877 MHz, is –76 dBc for one carrier and –75 dBc for two carriers, measured from the first adjacent channel. The AD9161's intermodulation distortion (IMD), for a 0-dB full-scale (FS) signal at 900 MHz, is –75 dBc, rising to just –71 dBc for a 0-dB FS signal at 1800 MHz. Noise spectral density for a single tone is just –157 dBm/Hz at 550 MHz, –155 dBm/Hz at 960 MHz, and –155 dBm/Hz at 1990 MHz.

For the AD9162, adjacent-channel power for 877 MHz output frequency is –79 dBc for one carrier and –76 dBc for two carriers, measured from the first adjacent channel. And it is –74 dBc for one carrier at 1987 MHz and –70 dBc for two carriers at 1990 MHz. IMD is –80 dBc at 900 MHz and –68 dBc at 1800 MHz.

The single-tone noise spectral density is somewhat lower than that of the AD9161: –168 dBm/Hz at 550 MHz, –167 dBm/Hz at 960 MHz, and –164 dBm/Hz at 1990 MHz. For a DAC frequency of 4 Gsamples/s and output frequency of 3.8 GHz, the single-sideband phase noise of the AD9162 is –119 dBc/Hz offset 1 kHz from the carrier, –125 dBc/Hz offset 10 kHz from the carrier, –135 dBc/Hz offset 100 kHz, and –144 dBc/Hz offset 1 MHz. mw

ANALOG DEVICES INC., One Technology Way, P. O. Box 9106, Norwood, MA 02062-9106; (781) 329-4700, www.analog.com

JACK BROWNE | Contributing Editor

Making the Best of Miniature Circuits

For circuits with miniature dimensions, this firm provides the expertise and equipment to fabricate micron-sized features on both rigid and flexible substrate materials.

MINIATURIZATION IS THE KEY to many successful applications, including pocket-sized radios and medical electronic solutions. While small components like planar antennas and inductive coils enable many small-scale electronic products to operate, making circuit structures and components with micron-sized features is (pardon the pun) no small feat.

Metrigraphics has been doing that for five decades. The company houses both the equipment and the expertise to fabricate micron-scale components and circuit structures with dimensions of 5 μm or less on hard and software substrate materials.

Micron-sized circuit features are usually associated with semiconductor devices, but Metrigraphics has been fabricating micron-scale circuit features for passive components, including induction coils and optical components. Miniature induction coils enable such applications as pill-sized ingestible medical biosensors, where the inductors provide an energy source for the sensors without need for a much larger battery.

The firm works with thin-film and flexible substrate materials, employing a blend of standard and proprietary processes to achieve fine feature resolution with high repeatability. Multilayer flexible circuits can be fabricated with as many as seven metallized layers and up to six substrate layers. Metallization processes include photolithography, plated metal deposition, and sputtered thin-film techniques.

DIVING INTO DIMENSIONS

Thin-film circuits are based on polished and as-fired ceramic substrates, in addition to polished sapphire and quartz glass substrates, in a range of thicknesses. The dielectric constants of these substrates range from 3.8 to 10.0 at 10 MHz with low loss tangents. For example, the loss tangent for a quartz glass substrate with dielectric constant of 3.8 at 10 MHz is just 0.000015 at 1 MHz. Conductor lines and spacing on thin-film substrates can be formed with precision of 0.050 mm and tolerance as good as ±0.005 mm.

Conductor widths can be maintained to a tolerance of ±0.005 mm. Conductors can be places within 0.200 mm of the edge of a substrate, allowing for the formation of extremely high-density, miniature circuits. For multilayer circuits, viaholes can also be tightly spaced, as close as ±0.05 mm from the center of one viahole to the center of another viahole, depending upon the diameters of the holes.

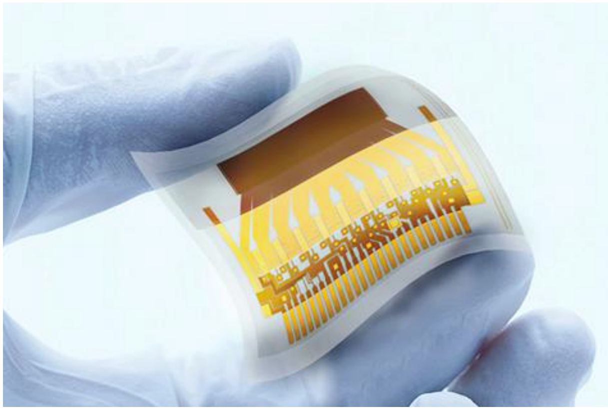

Miniature circuit dimensions can be achieved on both rigid and flexible, bendable circuits such as this.

Metrigraphics has fabricated a wide array of planar and 3D circuits and circuit structures for RF, medical, and optical applications. The company has fabricated over 160 different induction coils for various applications, including biomedical use. These are single- or multiple-layer structures (*see figure*) in round and square configurations with different metallizations and substrate materials.

Coil traces as fine as 3 μm have been formed repeatably on some of these coils, as a demonstration of fabrication capabilities that extend from the prototype stage to full production. Visitors to the company's website can learn more about the various dielectric and metallization combinations and dimensional tolerances for different structures and circuit configurations. mw

METRIGRAPHICS, 1001 Pawtucket Blvd., Lowell, MA 01854; (800) 261-2557, www.metrigraphicsllc.com

Mini-Circuits Trivia Game

WIN AN iPad®

Visit Booth 215 at EDI CON to enter!

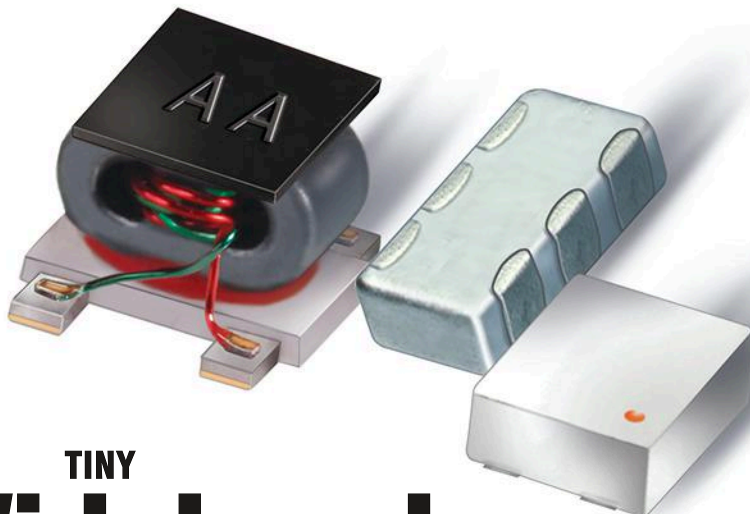

TINY

Wideband Transformers & Baluns!

NOW! **4 kHz - 18 GHz** From 99¢ ea.(qty.20)

To support an even wider range of applications, Mini-Circuits tiny surface-mount transformers and baluns now cover frequencies from 4 kHz up to 18 GHz! Our latest designs achieve consistent performance across very wide frequency bands, and our baluns have demonstrated great utility for use with chipsets. With over 250 trusted models in stock representing a wide selection of circuit topologies and impedance ratios, chances are, we have a solution for your needs!

Our Low Temperature Co-Fired Ceramic (LTCC) models provide reliable performance in tough operating conditions, tiny size – as small as 0805 – and very low cost. All core-and-wire models are available with our exclusive Top Hat® feature, improving pick-and-place accuracy and throughput. We even manufacture our own transmission wire under rigorous control and use all-welded connections to ensure reliability and repeatability you can count on.

Visit minicircuits.com and use **Yoni2®**, our patented search engine to search our entire model database by performance criteria and find the models that meet your requirements. Order today and have them in hand as soon as tomorrow! Cost-effective custom designs and simulations with fast turnarounds are just a phone call away!

TC
0.15" x 0.15"

NC
0.08 x 0.05"
Ceramic

NCR2
0.08 x 0.10"
Ceramic

RoHS compliant.

Mini-Circuits®

www.minicircuits.com P.O. Box 350166, Brooklyn, NY 11235-0003 (718) 934-4500 sales@minicircuits.com

528 rev AEDI

JACK BROWNE | Contributing Editor

OCXO Trims Phase Noise and Power Consumption

This OCXO delivers outstanding frequency stability with several levels of available phase-noise performance and industry-low power consumption.

MINIMIZING POWER CONSUMPTION is vital to many applications where the power supply is limited, such as in portable and/or battery-based electronic devices. Saving power, however, can prove to be costly in terms of performance for some components. Oven-controlled crystal oscillators (OCXOs), for instance, can exhibit degraded stability and phase noise at lower power levels.

Fortunately, the model LP102 OCXO from Bliley Technologies is designed for outstanding stability and phase noise, all the while consuming a mere 135 mW of power during steady-state operation. The OCXO is available with sinewave or HCMOS outputs (with 10-ns rise/fall time) at frequencies from 10 to 50 MHz, and with initial accuracy of ±10 ppb.

The LP102 is a low-phase-noise OCXO available with sinewave or HCMOS output signals and low steady-state power consumption.

OCXOs like the model LP102 *(see figure)* are critical to maintaining frequency stability and precise timing in analog and digital circuits and systems. The basic design achieves excellent crystal-resonator stability with changes in temperature by maintaining the crystal in a temperature-controlled enclosure. The penalty for enhanced temperature stability is the increased power consumption required to control the temperature of the crystal chamber.

As expected, the LP102 consumes an increased amount of power during startup (350 mW) when it must stabilize the temperature of the crystal chamber. However, once this is accomplished (typically in one minute or less), the steady-state power consumption is only 135 mW—remarkably low for an OCXO of any kind, as they are usually rated in terms of watts of power consumption.

The LP102 in no way compromises its performance for the low power consumption. The phase-noise performance is specified separately for sinewave and HCMOS outputs, as well as for two different temperature ranges.

By way of example: For sinewave outputs from −20 to +70°C, the static phase noise is typically −95 dBc/Hz offset 1 Hz from the carrier, −125 dBc/Hz offset 10 Hz, −162 dBc/Hz offset 1 kHz, and −165 dBc/Hz offset 10 kHz.

For sinewave outputs from −40 to +85°C, the phase noise is typically −90 dBc/Hz offset 1 Hz from the carrier, −120 dBc/Hz offset 10 Hz, −158 dBc/Hz offset 1 kHz, and −162 dBc/Hz offset 10 kHz.

For HCMOS outputs from −20 to +70°C, the static phase noise is typically −95 dBc/Hz offset 1 Hz from the carrier, −125 dBc/Hz offset 10 Hz from the carrier, −152 dBc/Hz offset 1 kHz from the carrier, and −155 dBc/Hz offset 10 kHz from the carrier.

For the wider temperature range of −40 to +85°C, the phase noise drops to −90 dBc/Hz offset 1 Hz, −120 dBc/Hz offset 10 Hz, −150 dBc/Hz offset 1 kHz, and also −150 dBc/Hz offset 10 kHz from the carrier.

Harmonic levels are −30 dBc or better, while spurious levels are −60 dBc or better. The LP102 low-power OCXO features 0.5 ppb/g acceleration sensitivity. It delivers +9-dBm output power into a 50-Ω load. The OCXO incorporates electronic frequency control for adjustments over a total frequency range of ±0.5 ppm and 10% tuning linearity.

The oscillator is designed for power supplies of +3.3 V dc ±5% and +5.0 V dc ±5% and an operating temperature range of −40 to +85°. Different grades of performance are available, such as frequency stability of ±25, 50, 75, or 100 ppb from −20 to +70°C and ±75 or 100 ppb from −40 to +85°C. mw

BLILEY TECHNOLOGIES, 2545 W Grandview Blvd., Erie, PA 16506; (814) 838-3571, *www.bliley.com*

Bidirectional Amplifier Handles 1,350 to 1,390 MHz

MODEL TTRM1081 is a bidirectional amplifier capable of boosting receive and transmit signals from 1,350 to 1,390 MHz. The L-band unit is designed with power-amplifier (PA) and low-noise-amplifier (LNA) circuits in the same compact housing; it is suitable for communications applications in unmanned aerial vehicles (UAVs) and military mesh networks. It provides typical output power of +43 dBm at 1-dB compression and typical saturated output power of +44 dBm. The typical transmit gain is 25 dB and typical receive gain is 10 dB. The LNA noise figure is typically 2 dB. The switching speed between receive and transmit amplification is typically 1 μs. The amplifier runs on voltages of +27 to +30 V dc and measures 3.33 × 2.69 × 0.65 in.

TRIAD RF SYSTEMS,
180 Tices Ln., Bldg. A, Ste. 107, East Brunswick, NJ 08816;
(855) 558-1001, e-mail: sales@triadrf.com, *www.triadrf.com*

Rack-Mount Amplifier Powers 6 to 18 GHz

SOLID-STATE CLASS AB LINEAR AMPLIFIER model BHE69189-50 delivers 50 W of clean output power from 6 to 18 GHz. Suitable for test and systems applications, the rack-mountable amplifier provides more than 40 W output power into a load with 2.0:1 VSWR while achieving 45-dB typical gain. Second and third harmonics are less than –12 and –22 dBc, respectively, while spurious levels are better than –60 dBc. The amplifier, which is open/short tested, runs on ac supplies of 85 to 265 V. It measures 19.0 × 22.0 × 5.25 in. with Type N female connections (and options for TNC and SMA connectors). The amplifier is designed for operating temperatures from –20 to +50°C and weighs 40 lb.

COMTECH PST,
105 Baylis Rd., Melville, NY 11747;
(631) 777-8900, *www.comtechpst.com*

Cloverleaf Antennas Reach 2.5 GHz

A LINE OF COMPACT CIRCULARLY POLARIZED ANTENNAS is available for use from 1.98 to 2.20 GHz, as well as for 2.30 to 2.50 GHz for military and commercial applications. The rugged Turbo Cloverleaf family of antennas features components in the classic cloverleaf radome style with omnidirectional radiation patterns. The radome enclosure measures just 2 in. on a side for ease of colocation. The antennas also have integrated 3-in. coaxial gooseneck assemblies with non-rotating RF connectors, SMA connectors for the lower-frequency units, and TNC connectors for the higher-frequency antennas. The waterproof antennas are available with left-handed circular polarization (LHCP) and right-handed circular polarization (RHCP), with more than 40-dB isolation between antennas with the different polarizations. As an example, model 1032-021 operates from 1.98 to 2.20 GHz with RHCP (model 1032-022 for LHCP) with 1.2-dBi gain and a black-chrome male SMA connector. Model 1032-024 operates from 2.3 to 2.5 GHz with RHCP (model 1032-025 with LHCP) with 1.2-dBi gain and a black-chrome TNC connector.
SOUTHWEST ANTENNAS, 8145 Ronson Rd., Ste. B, San Diego, CA 92111; (858) 277-3300, e-mail: sales@southwestantennas.com, *www.southwestantennas.com*

VCOs Tune from 10 MHz to 11 GHz

COVERING BANDS FROM 10 MHz TO 11 GHz, a line of more than 60 models of voltage-controlled oscillators (VCOs) is available from stock for immediate shipping. The VCOs are designed to meet MIL-STD-202 environmental test conditions for shock, vibration, and temperature cycling, and include models with phase-noise performance as good as –125 dBc/Hz offset 10 kHz from the carrier. They provide output power from 0 to +12.5 dBm and operate on voltages from 0 to +20 V dc. The oscillators are available in hermetic surface-mount-technology (SMT) packages with gold-plated mounting surfaces and can be used at operating temperatures from –40 to +85°C.
FAIRVIEW MICROWAVE, 1130 Junction Dr., Ste. 100, Allen, TX 75013; (972) 649-6678; *www.fairviewmicrowave.com*

Miniature Signal Generator Spans 6 to 18 GHz

MODEL LMS-183DX is a Lab Brick compact, modular signal generator with a frequency range of 6 to 18 GHz. It provides output-level control from +10 to –70 dBm from 6 to 13 GHz, and from +10 to -55 dBm from 13 to 18 GHz. It weighs less than 1 lb. and measures 4.90 × 3.14 × 1.59 in. (124 × 80 × 40 mm) with maximum harmonics of –25 dBc. The signal generator, which performs phase-continuous frequency sweeps, is controlled and powered by means of a Universal Serial Bus (USB) connector. P&A: $3499; 3 weeks.

VAUNIX TECHNOLOGY CORP., 7 New Pasture Rd., Newburyport, MA 01950; (978) 662-7839, e-mail: Vaunix-Sales@vaunix.com, *www.vaunix.com*

Power Dividers Cover Multiple Bands to 6 GHz

A LINE OF RF/MICROWAVE POWER DIVIDERS has been extended with the addition of broadband models operating from UHF through ISM bands. Models in the 80X-X-3.250WWP line are available with Type N and SMA connectors in 2-, 4-, 8-, 16-, and 32-way configurations with performance optimized for use from 500 MHz to 6 GHz, and at power levels of 30 W and more. The rugged components are IP67-rated for indoor and outdoor use. Models are also available with BNC and TNC coaxial connectors.
MECA ELECTRONICS INC., Denville, NJ 07834; (866) 444-6322, e-mail: sales@e-MECA.com, *www.e-MECA.com*

TEST CABLES *up to 40 GHz!*

Reliability You Can Trust... *from* $68.95 ea. (qty.1-9)

Why do 10,000 customers trust Mini-Circuits test cables? Because they simply don't fail! Our test cables have been performance qualified to 20,000 flexures* and come backed by our 6-month product guarantee**, so you can be confident you're getting rugged construction, reliability, and repeatable performance you can depend on. Whether you're performing production test, burn-in, over-temperature testing, hi-rel testing – you name it – chances are there's a Mini-Circuits test cable for your application in stock, ready for immediate shipment. Order some for your test setup at minicircuits.com today, and you'll quickly find that consistent long-term performance, less retesting and fewer false rejects really add up to bottom-line savings, test after test!

	Model Family	Capabilities	Freq. (GHz)	Connectors†
	KBL	Precision measurement, including phase, through 40 GHz	DC-40	2.92mm
	CBL- 75+	Precision 75Ω measurement for CATV and DOCSIS® 3.1	DC-18	N, F
	CBL	All-purpose workhorse cables for highly-reliable, precision 50Ω measurement through 18 GHz	DC-18	SMA, N
	APC	Crush resistant armored cable construction for production floors where heavy machinery is used	DC-18	N
	ULC	Ultra-flexible construction, highly popular for lab and production test where tight bends are needed	DC-18	SMA
	FLC	Flexible construction and wideband coverage for point to point radios, SatCom Systems through K-Band, and more!	DC-26	SMA
NEW!	VNAC	Precision VNA cables for test and measurement equipment through 40 GHz	DC-40	2.92mm (M to F)

* All models except VNAC-2R1-K+

** Mini-Circuits will repair or replace your test cable at its option if the connector attachment fails within six months of shipment. This guarantee excludes cable or connector interface damage from misuse or abuse.

† Various connector options available upon request.

Contact apps@minicircuits.com to discuss your special requirements.

Mini-Circuits®

www.minicircuits.com P.O. Box 350166, Brooklyn, NY 11235-0003 (718) 934-4500 sales@minicircuits.com

This index is provided as an additional service by the publisher, who assumes no responsibility for errors or omissions.

Subscription Assistance and Information:
(ISSN 0745-2993)
Microwaves & RF is published monthly. Microwaves & RF is sent free to individuals actively engaged in high-frequency electronics engineering. In addition, paid subscriptions are available. Subscription rates for U.S. are $95 for 1 year ($120 in Canada, $150 for International). Published by Penton Media, Inc., 9800 Metcalf Ave., Overland Park, KS 66212-2216. Periodicals Postage Paid at Kansas City and additional mailing offices. POSTMASTER: Send change of address to Microwaves & RF PO Box 2100, Skokie, IL 60076-7800. For paid subscription information, please contact Microwaves & RF at PO Box 2100, Skokie IL 60076-7800. Canada Post Publications Mail agreement No. 40612608. Canada return address: IMEX Global Solutions PO Box 25542, London ON N6C 6B2.

Get a piece of the ARRA pie...

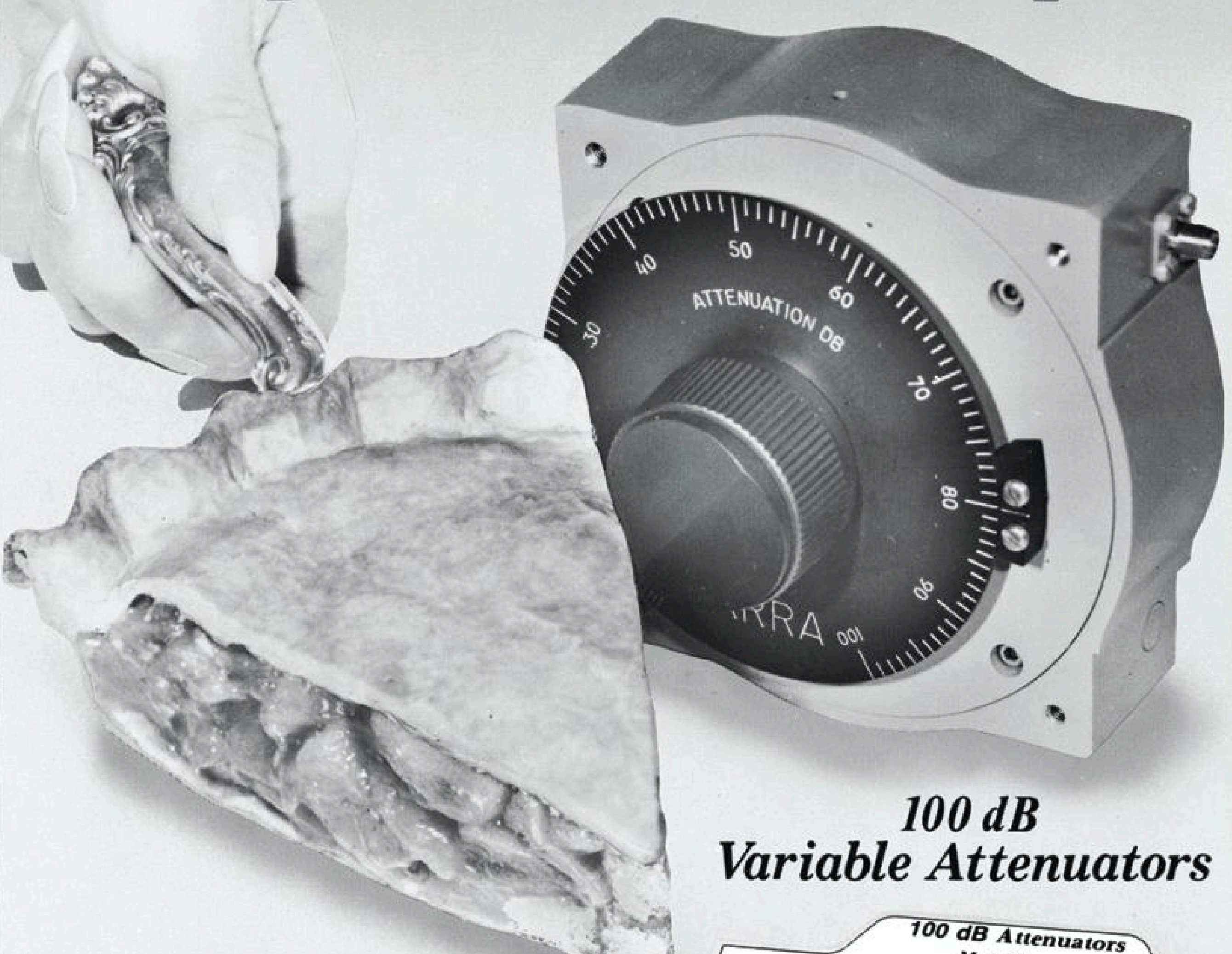

100 dB Variable Attenuators

100 dB Attenuators
Mmmm....

Freq Range	Atten vs Freq · dB	Model #
500 - 1000 MHz	1.5	2952 - 100
900 - 1300 MHz	0.75	2-3952 - 100
1000 - 2000 MHz	1.5	3952 - 100X
2000 - 4000 MHz	1.5	4952 - 100 X
4000 - 8000 MHz	1.5	5952 - 100X

Insertion loss - 6 dB
VSWR - 1.5
Power - 15 cw
Temperature -30 to +120 C

Now, you can have your pie and eat it too! Only from ARRA! Four models that cover the 500 to 8000 MHz frequency range! Available in lower attenuation ranges. *Customerized to your requirements with little or no additonal charge.* Top performance. Super dial accuracy.

- Direct reading dial
- Extremely high reliability
- Non-contacting movable parts (our special recipe)
- High power version available (up to 200 W)
- Usage will not change calibration
- Attenuation will not vary with temperature
- Excellent phase characteristics
- Type N standard SMA connectors available

Applications include:
•TACAN •DME/IFF •Lab standards •Altimeter
Or any other requirements needing high attenuation and accurate dial reading.

Visit our website at www.arra.com
E-Mail: sales@arra.com

Some of the best attenuator recipes you can find are cooking at ARRA right now! Send for your copy today and get a piece of the ARRA pie.

. . . the last word in variable attenuators

ARRA INC.

15 Harold Court • Bay Shore NY 11706-2296

Tel 631-231-8400 Fax 631-434-1116